DETERMINATION OF SIALIC ACID BY USING PLASMONIC NANOPARTICLES

A THESIS SUBMITTED TO
THE GRADUATE SCHOOL OF NATURAL AND APPLIED SCIENCES
OF
MIDDLE EAST TECHNICAL UNIVERSITY

BY

EDA AKIN

IN PARTIAL FULFILLMENT OF THE REQUIREMENTS
FOR
THE DEGREE OF MASTER OF SCIENCE
IN
CHEMISTRY

JUNE 2022

Approval of the thesis:

DETERMINATION OF SIALIC ACID BY USING PLASMONIC NANOPARTICLES

submitted by **EDA AKIN** in partial fulfillment of the requirements for the degree of **Master of Science** i**n Chemistry, Middle East Technical University** by,

Prof. Dr. Halil Kalıpçılar
Dean, Graduate School of **Natural and Applied Sciences** _____

Prof. Dr. Özdemir Doğan
Head of the Department, **Chemistry** _____

Prof. Dr. Mürvet Volkan
Supervisor, **Chemistry, METU** _____

Prof. Dr. Gülay Ertaş
Co-Supervisor, **Chemistry, METU** _____

Examining Committee Members:

Prof. Dr. Orhan Atakol
Chemistry, Ankara University _____

Prof. Dr. Mürvet Volkan
Chemistry, METU _____

Prof. Dr. Gülay Ertaş
Chemistry, METU _____

Prof. Dr. Murat Kaya
Chemical Engineering, Atılım University _____

Assoc. Prof. Dr. Ezel Boyacı
Chemistry., METU _____

Date: 22.06.2022

I hereby declare that all information in this document has been obtained and presented in accordance with academic rules and ethical conduct. I also declare that, as required by these rules and conduct, I have fully cited and referenced all material and results that are not original to this work.

Name Last name : Eda Akın

Signature :

ABSTRACT

DETERMINATION OF SIALIC ACID BY USING PLASMONIC NANOPARTICLES

Akın, Eda
Master of Science, Chemistry
Supervisor : Prof. Dr. Mürvet Volkan
Co-Supervisor: Prof. Dr. Gülay Ertaş

June 2022, 67 pages

Sialic acids are an important sub-group of nine carbon acidic sugars. Sialic acid plays a significant role in mediating and modulating a variety of physiological activities due to its widespread distribution in human body. Several pathogens and toxins also bind to sialic acid, change its level and signal pathological conditions. The identification and quantification of sialic acid levels are also significant for early detection of many diseases such as breast and colon cancer.

In this study, sialic acid determination in the form of N-acetylneuraminic acid (Neu5Ac) and N-glycolylneuraminic acid (Neu5Gc) was aimed. Serotonin has specific affinity for sialic acid. Hence a novel detection strategy, which is based on the sialic acid-induced aggregation of serotonin functionalized gold nanoparticles, was proposed. Serotonin was bonded on gold nanoparticles utilizing two crosslinkers with different lengths: 1-Ethyl-3-(3-dimethylaminopropyl) carbodiimide / N-Hydroxysuccinimide (EDC/NHS) and Dithiobis(succinimidylpropionate) (DSP). Progressive additions of various sialic acid concentrations resulted in distinct color changes on serotonin modified gold nanoparticle probes (DSP-AuNPs@SER and EDC/NHS-AuNPs@SER) from red to purple and blue which indicates the affinity-

aggregation. At optimal conditions while using EDC/NHS-AuNPs@SER probe, the absorbance ratio (A_{625}/A_{521}) was linear with respect to N-acetylneuraminic acid concentrations ranging from 300 to 750 µM. The limit of quantification 257.5 µM was achieved for Neu5Ac. Furthermore, at optimal conditions while using DSP-AuNPs@SER probe, the absorbance ratio (A_{625}/A_{521}) was linear with respect to N-acetylneuraminic acid concentrations ranging from 16.7 to 58.3 µM . The limit of quantification 10.0 µM was achieved for Neu5Ac. Moreover, at optimal conditions while using DSP-AuNPs@SER probe, the absorbance ratio (A_{625}/A_{521}) was linear with respect to N-glycolylneuraminic acid concentrations ranging from 8.3 to 58.3 µM . The limit of quantification 17.3 µM was calculated for Neu5Gc. Both probes were successful only for sialic acid among glucose, fructose, mannose, lactose, sucrose, and maltose. Applications of serotonin assembled gold nanoparticles in human serum to determine total serum sialic acid are in progress.

Keywords: Gold Nanoparticle, Sialic Acid, N-acetylneuraminic acid, N-glycolylneuraminic acid, Colorimetric Determination

ÖZ

PLAZMONİK NANOPARÇACIKLAR KULLANILARAK SİALİK ASİT TAYİNİ

Akın, Eda
Yüksek Lisans, Kimya
Tez Yöneticisi: Prof. Dr. Mürvet Volkan
Ortak Tez Yöneticisi: Prof. Dr. Gülay Ertaş

Haziran 2022, 67 sayfa

Dokuz karbon asidik şekerden oluşan bir grup olan sialik asitler, hücre yüzeyindeki glikanların terminal şekerleri olarak bulunur. Sialik asit, yaygın dağılımı ve konumu nedeniyle çeşitli fizyolojik aktivitelere aracılık etmede ve modüle etmede önemli bir role sahiptir. Sialik asit seviyesindeki değişiklikler patolojik durumlara da işaret eder çünkü çoğu patojen ve toksin sialik aside kolaylıkla bağlanır. Sialik asit seviyelerinin tanımlanması ve nicelenmesi, meme ve kolon kanseri gibi birçok hastalığın erken teşhisi için de çok önemlidir.

Bu çalışmada N-asetilnöraminik asit ve N-glikolilnöraminik asit formunda sialik asit tayini amaçlanmıştır. Serotonin, sialik asit için spesifik afiniteye sahiptir. Bu nedenle, serotonin ile işlevselleştirilmiş altın nanoparçacıklarının sialik asit kaynaklı toplanmasına dayanan yeni bir saptama stratejisi önerilmiştir. Serotonin, farklı uzunluklarda iki farklı bağlayıcı kullanılarak altın nanoparçacıklar üzerine bağlandı: 1-Etil-3-(3-dimetilaminopropil) karbodiimid / N-Hidroksisüksinimit (EDC/NHS) ve Ditiobis(süksinimidilpropionat) (DSP). Çeşitli sialik asit derişimlerinin aşamalı olarak eklenmesi, Serotonin ile modifiye edilmiş altın nanoparçacık problarında (DSP-AuNPs@SER ve EDC/NHS-AuNPs@SER) kırmızıdan mora ve afinite

toplanmasını gösteren maviye doğru belirgin renk değişiklikleriyle sonuçlandı. EDC/NHS-AuNPs@SER probu kullanılırken optimal koşullarda, absorbans oranı (A_{625}/A_{521}) 300 ila 750 µM arasında değişen N-asetilnöraminik asit konsantrasyonlarına göre doğrusaldı. Neu5Ac için 257.5 µM miktar belirleme sınırına ulaşıldı. Ayrıca, DSP-AuNPs@SER probu kullanılırken optimal koşullarda, absorbans oranı (A_{625}/A_{521}), 16.7 ila 58.3 µM arasında değişen N-asetilnöraminik asit konsantrasyonlarına göre doğrusaldı. Neu5Ac için 10.0 µM miktar belirleme sınırına ulaşıldı. Ayrıca, DSP-AuNPs@SER probu kullanılırken optimal koşullarda, absorbans oranı (A_{625}/A_{521}), 8.3 ila 58.3 µM arasında değişen N-glikolilnöraminik asit konsantrasyonlarına göre doğrusaldı. Neu5Gc için miktar belirleme sınırı 17.3 µM hesaplandı. Her iki prob içinde yalnızca glukoz, fruktoz, mannoz, laktoz, sakaroz ve maltoz arasında sialik asit için başarılı olmuştur. Toplam serum sialik asidini belirlemek için insan serumunda serotonin ile birleştirilmiş altın nanoparçacıkların uygulama çalışmalarına devam edilmektedir.

Anahtar Kelimeler: Altın Nanoparçacıklar, Sialik Asit, N-asetilnöraminik asit, N-glikolilnöraminik asit, Kolorimetrik Tayin.

To My Beloved Family

ACKNOWLEDGMENTS

The author wishes to express her deepest gratitude to her supervisor Prof. Dr. Mürvet Volkan for her invaluable advice, unwavering support, and patience throughout the research. Her plentiful experience for both academic and social life are gratefully appreciated. This thesis would not have been possible without her guidance.

The author would like to express her greatest appreciation to Dr. Yeliz Akpınar for her invaluable contribution. Her insightful comments and practical suggestions have been essential during the study. Her unwavering support is greatly appreciated.

The author would like to thank Prof. Dr. Gülay Ertaş for sharing her extensive knowledge and plentiful experience about the aspects of both academic and social life.

The author expresses her gratefulness to her lab mate, Begüm Avcı for their precious friendship. Her knowledge, support, and help throughout this study are gratefully acknowledged.

The author would like to thank Sezin Atıcı Özdemir and Canan Höçük Özkan for their support.

The author would also like to thank her sincere friends Dr. Merhdad Forough and Dr. Zübeyir Elmazoğlu for their valuable friendship and support.

The author wishes to acknowledge the great love and support of her beloved family, Filiz Akın and Erhan Akın, for providing her with unfailing support and continuous encouragement throughout her life. This accomplishment would not have been possible without them.

TABLE OF CONTENTS

ABSTRACT v

ÖZ……..... vii

ACKNOWLEDGMENTS x

TABLE OF CONTENTS xii

LIST OF TABLES xvi

LIST OF FIGURES xvii

LIST OF ABBREVIATIONS xx

CHAPTERS

1 INTRODUCTION 1

1.1 Nanotechnology 1

1.2 Nanoparticles 1

1.2.1 Plasmonic Nanoparticles 1

1.2.2 Gold Nanoparticles 2

1.2.3 Synthesis of Gold Nanoparticles 4

1.3 Sialic Acid 4

1.3.1 Importance of Sialic Acid Determination 5

1.3.2 Methods for Determination of Sialic Acid 6

1.4 Serotonin 8

1.4.1 The Affinity of Serotonin Towards Sialic Acid 9

1.5 Aim of the Study 9

2 EXPERIMENTAL 11

2.1 Chemicals and Reagents 11

2.1.1 Synthesis of Gold Nanoparticles.....11
2.1.2 Serotonin Addition to Gold Nanoparticles via EDC/NHS Coupling.....11
2.1.3 Sialic Acid Determination using EDC/NHS-AuNPs@SER Probe.....12
2.1.4 Functionalization of DSP onto Surface of Gold Nanoparticles.....12
2.1.5 Serotonin and Sialic Acid Addition to DSP-AuNPs.....12
2.1.6 Functionalization of DSP onto Surface of Gold Nanoparticles by Titration Method.....12
2.1.7 Serotonin Addition to DSP-AuNPs.....12
2.1.8 Sialic Acid Determination to AuNPs-DSP@SER probe.....13
2.1.9 Selectivity Studies.....13
2.2 Instrumental.....13
2.2.1 Ultrasonic Bath Sonicator.....13
2.2.2 Vortex Mixer.....13
2.2.3 Nutating Mixer.....13
2.2.4 pH Meter.....14
2.2.5 Centrifuge.....14
2.2.6 Ultraviolet-Visible Spectrophotometry.....14
2.2.7 Attenuated Total Reflection Fourier-Transform Infrared Spectrometer.....14
2.2.8 Dynamic Light Scattering.....14
2.2.9 Scanning Electron Microscopy.....15
2.3 Procedures.....15
2.3.1 Synthesis of Gold Nanoparticles.....15
2.3.2 Serotonin Addition to Gold Nanoparticles via EDC/NHS Coupling.....16
2.3.3 Sialic Acid Determination to EDC/NHS-AuNPs@SER Probe.....16

2.3.4 Functionalization of DSP onto AuNPs Surface 17
2.3.5 Serotonin and N-acetylneuraminic Acid Addition to DSP-AuNPs 18
2.3.6 Optimization of the Amount of DSP to be used in the Surface Coating of AuNPs 18
2.3.7 Optimization of the amount of Serotonin to be used in the surface coating of AuNPs 19
2.3.8 Sialic Acid Determination using DSP-AuNPs@SER Probe 20
2.3.9 Selectivity 21
3 RESULTS AND DISCUSSION 23
3.1 Synthesis of Gold Nanoparticles 23
3.2 Serotonin Addition to AuNPs via EDC/NHS Coupling 29
3.3 Sialic Acid Determination using EDC/NHS-AuNPs@SER Probe 31
3.3.1 Neu5Ac Determination using EDC/NHS-AuNPs@SER Probe 33
3.3.2 Neu5Gc Determination using EDC/NHS-AuNPs@SER Probe 36
3.4 The Functionalization of DSP on the AuNPs Surface 37
3.5 Serotonin Addition to DSP-AuNPs and Neu5Ac Determination using DSP-AuNPs@SER Probe 38
3.6 Optimization of the Amount of DSP to be used in the Surface Coating of AuNPs 40
3.7 Optimization of the Amount of Serotonin to be used in the Surface Coating of AuNPs 42
3.8 Sialic Acid Determination using DSP-AuNPs@SER Probe 46
3.8.1 Neu5Ac Determination using DSP-AuNPs@SER Probe 46
3.8.2 Neu5Gc Determination using DSP-AuNPs@SER Probe 49
3.9 Selectivity Studies 51

4 CONCLUSION.....55

REFERENCES 59

LIST OF TABLES

TABLES

Table 2.1. The Amounts of DSP used for titration 19
Table 2.2. DSP:SER mol ratio 20
Table 3.1 Mole ratios of Au^{3+}/Citrate in gold nanoparticle solutions 23
Table 3.2 Parameters used in temperature and time optimizations of citrate stabilized gold nanoparticle synthesis 24
Table 3.3 Temperature optimization of gold nanoparticle synthesis by using 1.575 x 10^{-6} mol of citric acid 26
Table 3.4. The statistical data obtained from calibration plot in Figure 3.12 35
Table 3.5 The final concentrations of N-acetylneuraminic acid 39
Table 3.6 The volumes and number of nmoles of titrant and DSP concentrations in the final aqueous solution containing 150 μL of AuNPs 41
Table 3.7 Mol ratio of DSP:SER 43
Table 3.8. The statistical data obtained from calibration plot in Figure 3.23 48
Table 3.9 The statistical data obtained from calibration plot in Figure 3.25 50

LIST OF FIGURES

FIGURES

Figure 1.1. LSPR of metal nanoparticles 2
Figure 1.2. Chemical Structures of N-acetylneuraminic Acid and N-glycolylneuraminic acid 5
Figure 1.3. Chemical Structure of Serotonin 8
Figure 1.4. Binding sites between Serotonin and N-acetylneuraminic Acid 9
Figure 1.5. The schematic of sialic acid sensor 10
Figure 3.1 The absorption spectra of citrate stabilized gold nanoparticles at different temperatures and times. 1 to 6 refers to solution numbers given in Table 3.2 25
Figure 3.2 The red color of gold nanoparticles 27
Figure 3.3. Size Distribution graph of gold nanoparticles 28
Figure 3.4. SEM images of gold nanoparticles 28
Figure 3.5. EDX analysis of AuNPs formed by reduction of sodium tetrachloroaurate dihydrate by trisodium citrate dihydrate 29
Figure 3.6 The chemical reaction scheme for the amine coupling. The carboxyl group is activated with EDC/NHS (1) followed by covalent attachment of Serotonin by its primary amine (2) 30
Figure 3.7 Absorption spectra of Neu5Ac addition to (a) EDC/NHS-AuNPs and (b) EDC/NHS-AuNPs@SER 31
Figure 3.8 The color of EDC/NHS-AuNPs@SER at pH from left to right 2.3, 5.4, 7.4 and 10.0, respectively 32
Figure 3.9 The color of EDC/NHS-AuNPs@SER solutions at pH from left to right 5.4 in the absence of Neu5Ac, at pH 5.4 in the presence of Neu5Ac, at pH 7.4 in the absence of Neu5Ac, at pH 7.4 in the presence of Neu5Ac, respectively. Reaction time was 5 min 33

Figure 3.10 Color scheme of EDC/NHS-AuNPs@SER after addition from 5 to 750 μM of Neu5Ac standard solutions, respectively 34
Figure 3.11 Red shift in the absorbance spectrum of EDC/NHS-AuNPs@SER probes in 5 to 750 μM of Neu5Ac standard solutions, respectively..... 34
Figure 3.12 Calibration plot obtained after addition of Neu5Ac..... 35
Figure 3.13 The color change of EDC/NHS-AuNPs@SER probes in 5 to 500μM of Neu5Gc standard solutions, respectively 36
Figure 3.14 EDC/NHS-AuNPs@SER probes in 5 to 500 μM of Neu5Gc standard solutions, respectively 37
Figure 3.15 The absorption spectrum of DSP-AuNPs 38
Figure 3.16 The color of DSP-AuNPs@SER at pH from left to right 2.0, 3.0, 4.0, 9.0, and 11.0, respectively 39
Figure 3.17 The absorption spectra of DSP-AuNPs@SER and DSP-AuNPs@SER probes in various concentrations of Neu5Ac standard solutions. 1 to 6 refers to solution numbers given in Table 3.5 40
Figure 3.18 Photometric titration curve: The rate of DSP hydrolysis was monitored at 260 nm following the additions of DSP standard solution to DIW containing 150 μL of AuNPs..... 42
Figure 3.19 The absorption spectra after Neu5Ac addition to DSP-AuNPs@SER with different SER concentrations..... 43
Figure 3.20 ATR-FTIR spectrum of DSP-AuNPs (a) expected peaks of DSP (b) expected peaks of SER (c) observed prominent peaks of DSP-AuNPs@SER (d) observed CO stretching belongs to DSP 45
Figure 3.21 Absorbance spectra of DSP-AuNPs@SER probe in (0.42 to 58.3 μM) concentration of Neu5Ac solutions 47
Figure 3.22 DSP-AuNPs@SER nanoparticles in 58.3, 50.0, 41.6, 33.0, 25.0, 16.7 and 8.30 μM Neu5Ac, respectively 47
Figure 3.23 Calibration plot for Neu5Ac measurements..... 48
Figure 3.24 Absorbance spectra of DSP-AuNPs@SER probes in (1.70 to 58.3 μM) concentration of Neu5Gc solutions 49

Figure 3.25 Calibration plot obtained after addition of Neu5Gc 50
Figure 3.26 (a)The color of change EDC/NHS-AuNPs@SER probe under the influence of sugars (glucose-1, fructose-2, galactose-3, mannose-4, sucrose-5, lactose-6 and maltose-7, respectively), sialic acid-9 and under the influence of sialic acid and mixture of sugars (All-10) (b)UV-Vis absorption spectra of EDC/NHS-AuNPs@SER probe under the influence of sugars, sialic acid and mixture of sugars 51
Figure 3.27 Absorbance ratio of EDC/NHS-AuNPs@SER under the influence of different sugars, SA, and the mixture of sugars (All) 52
Figure 3.28 Absorption spectra of DSP-AuNPs@SER probe under the influence of sugars, sialic acid and mixture of sugars..... 53
Figure 3.29 (a) the color of DSP-AuNPs@SER probe in control, glucose, fructose, galactose, mannose, sucrose, lactose, maltose, SA and mixture of sugars ALL, respectively (b) The bar graph of absorbance ratios (A_{625}/A_{521}) of DSP-AuNPs@SER with different sugars, SA and mixture of sugars (ALL)..... 54

LIST OF ABBREVIATIONS

ABBREVIATIONS	
ATR-FTIR	Attenuated total reflection Fourier-transform infrared
AuNPs	Gold nanoparticles
DLS	Dynamic Light Scattering
DSP	Dithiobis(succinimidylpropionate)
DSP-AuNPs	DSP functionalized gold nanoparticles
DSP-AuNPs@SER	Serotonin modified DSP-AuNPs
EDC	1-Ethyl-3-(3-dimethylaminopropyl) carbodiimide
EDC/NHS-AuNPs@SER	Serotonin modified gold nanoparticles via EDC/NHS
LDR	Linear dynamic range
LOQ	Limit of quantification
LSPR	Localized surface plasmon resonance
NHS	N-Hydroxysuccinimide
Neu5Ac	N-acetylneuraminic acid
Neu5Gc	N-glycolylneuraminic acid
UV-VIS	Ultraviolet-Visible
SA	Sialic Acid
SEM	Scanning Electron Microscope
SER	Serotonin
SERS	Surface-enhanced Raman scattering

TSA	Total sialic acid

CHAPTER 1

INTRODUCTION

1.1 Nanotechnology

The nanotechnology discipline plays a crucial role for the control or manipulate of matter at nanoscale [1]. The characteristics of materials at the nanoscale differ from those of bulk materials. Regardless of their size, bulk materials have consistent physical properties, whereas nanomaterials have unique size dependent physical and chemical properties [2]. They exhibit unique electrical, optical, magnetic, chemical, and mechanical properties [3]. Therefore, nanomaterials are widely used in different research areas that combines scientific branches from chemistry, biology, medicine, and molecular engineering to open new possibilities of application [4].

1.2 Nanoparticles

1.2.1 Plasmonic Nanoparticles

Plasmonic nanoparticles, including gold, silver, and platinum, are discrete metallic nanoparticles with distinctive optical properties [5]. Light interacts with nanoparticles much smaller than the incident wavelength, as shown in Figure 1.1. The conduction electrons on the nanoparticle surface undergo a collective oscillation called surface plasmon when excited by light at specific wavelengths. Since the fluctuation of surface electrons is restricted to a nanoparticle, a localized surface plasmon (LSPR) is formed [6]. The LSPR can create an intense electric field close to a particle surface resonance. The electric field forces surface electrons to flow in

one direction, forming a dipole that can shift orientation in response to the electric field [7]. The size, shape, and aggregation state of nanoparticles influence the amplitude and frequency of resonance; hence, the ability to design properties makes plasmonic nanoparticles more widespread [8].

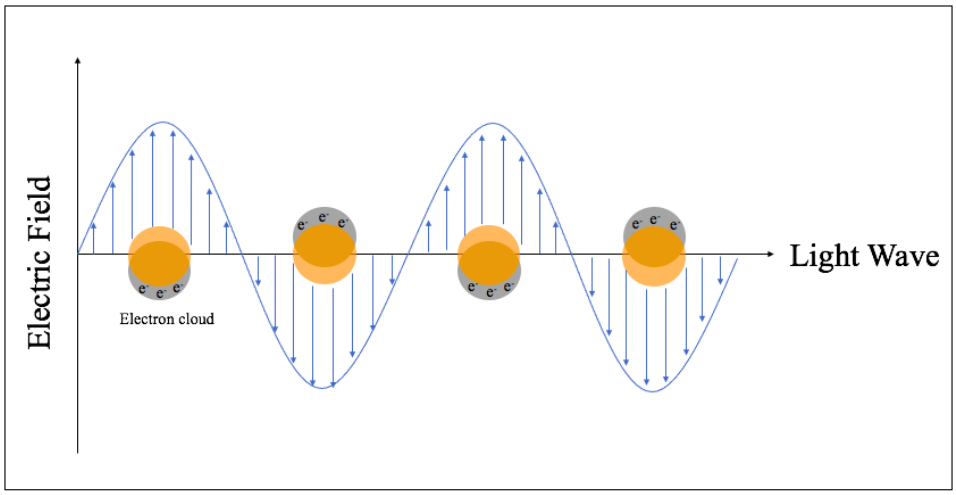


Figure 1.1. LSPR of metal nanoparticles

1.2.2 Gold Nanoparticles

Metallic nanoparticles have specialty with appropriate functional groups, and they can be manipulated to bind with ligands, antibodies, and drugs [9].

Among the different types of metallic nanoparticles, gold nanoparticles (AuNPs) remain one of the fascinating nanomaterials due to their unique characteristics which are easy to synthesize, allowing control over the physicochemical features, high binding affinity to thiols, disulfides and amines, distinctive tunable optical properties, high X-ray absorption coefficient and unique electronic properties [10,11].

As a result, their extraordinary physical and chemical properties make gold nanoparticles excellent for various applications including drug delivery, therapeutics, diagnostics, chemical sensing, imaging, and catalysis fields [12,13].

Gold nanoparticles have also drawn much attention in electrochemical fields because of their large surface area, high chemical stability, good biocompatibility, and ability to facilitate electron transfer between biomolecules and electrodes [14,15]. Functionalized gold nanoparticles can also be integrated into electrochemical techniques to improve their selectivity and sensitivity [16].

The shape-related optoelectronic properties, large surface-to-volume ratio, excellent biocompatibility, and low toxicity properties make gold nanoparticles ideal tools in biosensor applications [17]. Forming stable bonds with mercapto and amino groups to create selective binding and the similarity in the dimensions of gold nanoparticles and biomolecules such as proteins and DNA are other advantages of gold nanoparticles. The ease of surface modification with a wide range of biomolecules allows for the development of new biosensor platforms with enhanced capabilities in detecting various analytes.

The extraordinary efficiency of plasmonic nanoparticles at absorbing and scattering light provides an advantage in many applications, including chemical and biological sensors [18]. Surface-Enhanced Raman Scattering (SERS) is widely used for chemical and biomolecular sensing. Gold nanoparticles are considered an ideal SERS substrate since localized surface plasmon resonance excitation in Au nanoparticles produces strong extinction and scattering spectra. The choice of metallic substrate is critical since the enhancements are highly dependent on its characteristics [19]. Gold nanoparticles have been used for numerous critical SERS applications [20].

Unlike most dyes and pigments, the color of nanoparticles can be tuned to optimize performance without changing the chemical composition of the material [21]. Aggregation, for example, causes a change in the size of the nanoparticles and affects the color of their solutions. Accordingly, functionalized gold nanoparticles with a

specific affinity for a particular analyte can be used for the colorimetric detection of different analyte species [12].

1.2.3 Synthesis of Gold Nanoparticles

Michael Faraday provided the first scientific publication on the production of colloidal gold by reducing chloroauric acid with phosphorous and described the optical properties of nanometer-scale metals in 1857 [22]. His method was used to synthesize a wide range of gold nanoparticles with different geometry, size, chemistry, and functionality for a long time.

Turkevich proposed a gold nanoparticle synthesis method based on reducing solvated gold salts by surface capping ligands [23]. Hauser E.A. and Lynn J.E. in 1940 used trisodium citrate ($Na_3C_6H_5O_7$) as a reducing agent in producing gold nanoparticles [23]. These two methods are the most common ones to synthesize gold nanoparticles nowadays.

Although the properties of colloidal gold have been investigated for over a 150 years ago, a wide range of gold nanoparticles have been synthesized with different physical and chemical properties in today [24].

1.3 Sialic Acid

Sialic acids are diverse group of nine carbon carboxylated monosaccharides [25]. In general, sialic acid occupy the terminal positions of the carbohydrate chains of glycoproteins and glycolipids [26].

These nine-carbon monosaccharides have a great diversity. N-acetylneuraminic acid (Neu5Ac) and its hydroxylated form, N-glycolylneuraminic acid (Neu5Gc) are the main representative and most abundant forms of sialic acid [27]. In terms of their chemical structures, the only difference between them is that Neu5Ac has an acetyl

group on the fifth carbon atom (C5) while Neu5Gc has a glycolyl group instead, as shown in Figure 1.2.

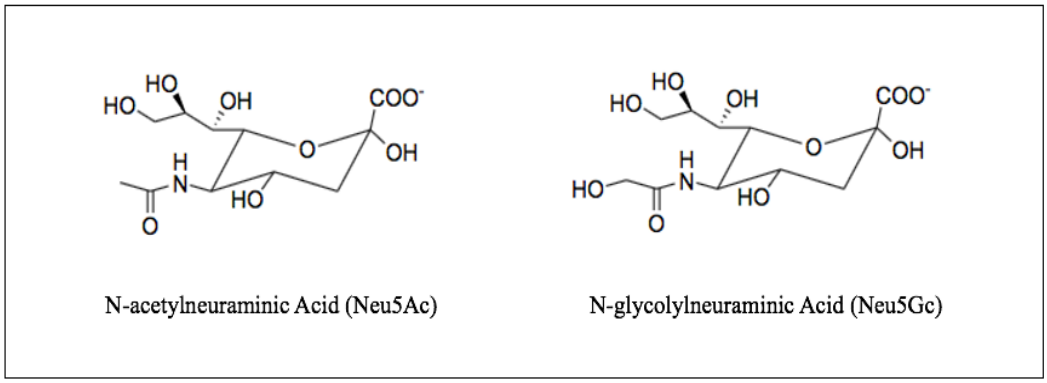


Figure 1.2. Chemical Structures of N-acetylneuraminic Acid and N-glycolylneuraminic acid

Sialic acids are found naturally on the surface of most eukaryotic cells and soluble proteins. They can be found in the free or bound form. It bounds typically to the terminal end of glycoproteins and glycolipid oligosaccharides [28].

The pathological pathways in human are able to synthesize Neu5Ac. Humans lack Neu5Gc due to the evolutionary loss of the cytidine monophosphate N-acetylneuraminic acid hydroxylase gene encoding the enzyme that converts Neu5Ac into Neu5Gc [29] . However, studies demonstrated that Neu5Gc can be found in human glycome due to certain types of diseases, especially breast and colon cancer [26]. Thus, sialic acid can be used as biomarker and its determination is significant.

1.3.1 Importance of Sialic Acid Determination

Sialic acid occupies the terminal position of carbohydrate chains and has a negative charge at physiological pH [30]. It is responsible for variable biochemical roles due to these unique structural properties. The most crucial function of sialic acid is the

mediation and modulation of various physiological and pathological activities, including cell-cell communication, immunological responses, cancer metastasis, and bacterial and viral infections [26]. In their interactions, the level and expression of sialic acids change unusually [31].

Approximately 80% of SA in serum is Neu5Ac [32]. The normal range of total sialic acid (TSA) level in serum/plasma is 1.58-2.22 mM whereas the free form of Neu5Ac only constituting 0.5-3 μM. In human glycoproteins and proportion of SA varies usually between 3% and 7% [32]. Notably, the higher amounts of free Neu5Ac are found in urine than in serum/plasma approximately 30-50% of the total sialic acid.

SA levels are elevated accordingly to the type disease. For instance, different increased levels of serum TSA have been observed in various patient groups suffering from advanced ovarian carcinoma, brain tumors, lung cancer, cervical cancer, etc. For instance, TSA amount obtained people suffering from stomach cancer is found 2.91±0.12 mM whereas the control amount is 1.98±0.06 mM [32]. Furthermore, the increase in SA has been observed to correlate positively with the level of metastasis. For example, TSA amount obtained people suffering from breast cancer at primary stage is found 1.77±0.35 mM whereas it is found as 2.04±0.33 mM in breast cancer with secondary growth [33]. Apart from cancer, SA levels are elevated in diabetes diseases. For Type I diabetes the TSA amount is found 1.85±0.26 mM, while healthy people have 1.98±0.67 mM TSA amount [34].

SA levels could be elevated in cancer patients before the occurrence of clinical symptoms [32]. Thus, identifying and quantifying sialic acid is significant for early detection of many diseases associated with chronic inflammation, including cancer, cardiovascular disease, and autoimmunity [11].

1.3.2 Methods for Determination of Sialic Acid

Since sialic acids have important functions in pathology and physiology, accurate, simple and rapid methods for sialic acid quantification and analysis have been

developed [35]. The high sensitivity of sialic acids in serum or plasma as a tumor marker has been reported in various cancerous conditions [36]. Quantification of total sialic acids or glycolipid-bound sialic acids in serum is helpful to improve the accuracy of clinical diagnoses and therapies. Detection methods have been established for quantification of sialic acids, including colorimetric assay [37], fluorometric assay [38], high performance liquid chromatography (HPLC) [39,40], fluorescence [41,42], and mass spectrometry (MS) [43]. All of them can detect sialic with commendable sensitivities. However, they also have some significant limitations. For instance, the conventional colorimetric methods have relatively longer assay time and include toxic organic reagents. High-skilled technicians for operations are required for chromatographic, mass spectrometric, and electrochemical methods, and they are relatively expensive.

The inclusion of gold nanoparticles in colorimetric methods has increased their application in analyzing a wide range of analytes. Thanks to the gold nanoparticles' unique optical and electronic properties, the color transitions of gold nanoparticles can be observed by the naked eye, which simplifies colorimetric detection. The stable and dispersed gold nanoparticles have a ruby red color. However, the color of gold nanoparticles changes from ruby red to purple and blue due to their agglomeration when ligands bind to gold nanoparticles. A UV-vis spectrophotometer is used to follow the corresponding changes in absorption spectra. The simplicity, speed, and low-cost advantages make the colorimetric methods using gold nanoparticles more popular. Therefore, there are many studies for their development for specific detection of analytes [44,45]. For instance, Jayeoye and coworkers developed a colorimetric method for sialic acid determination [31]. The method was based on the specific sialic acid induced aggregation of 3-aminophenyl boronic acid assembled on dithiobis (succinimidylpropionate) functionalized gold nanoparticles. At optimal conditions, the absorbance ratio A_{700}/A_{520} was linear with sialic acid concentrations between 0.08 and 0.25 mM. A limit of detection of 35 μM was achieved.

Sankoh and coworkers developed a colorimetric method for sialic acid determination based on the aggregation of 4-mercaptophenylboronic acid functionalized gold nanoparticles [46]. Their colorimetric sensor provided good analytical performances with a linear dynamic range of 80 μM to 2.00 mM and a 68 μM limit of detection without any effect from possible interferences and sample matrix.

1.4 Serotonin

Serotonin (5-hydroxytryptamine, 5-HT), as shown in Figure 1.3, is mainly found inside the brain and is a crucial monoamine neurotransmitter to carrying signals between the nerve cells throughout the body [47]. It plays a vital role in controlling the sensory information in the central nervous system [48].

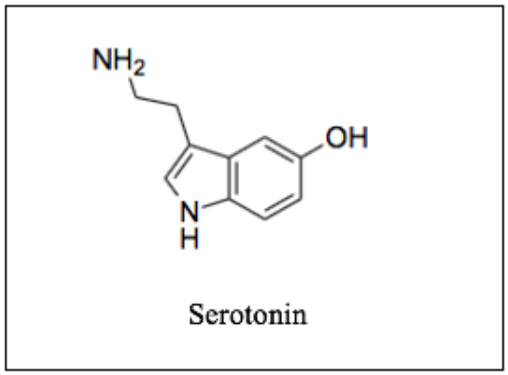


Figure 1.3. Chemical Structure of Serotonin

Although serotonin acts as a critical hormone for human well-being and happiness, it also influences physiological properties such as cardiovascular, gastrointestinal, platelet, smooth muscular contraction, and uterine smooth muscle [49,50]. The irregular serotonin concentration is related with several disorders, including depression, anxiety, and migraines, as well as toxic and potentially fatal effects [47].

1.4.1 The Affinity of Serotonin Towards Sialic Acid

In physiological and pathological conditions, sialic acid recognizes a wide range of biomolecules such as serotonin. The affinity of serotonin towards Neu5Ac-containing glycolipids and glycoproteins was reported first time by Ochoa and Bangham in 1976 [51]. In 1982, Sturgeon and coworkers published specific retention of Neu5Ac-containing glycoconjugates in the serotonin-immobilized gel. They also emphasized the presence of an N-acetyl group and a side chain (C7-C9) of Neu5Ac are necessary for binding to serotonin, as shown in Figure 1.4 [52,53]. Therefore, serotonin could be an excellent candidate as a ligand to determine sialic acid, exclusively due to the affinity between sialic acid and serotonin.

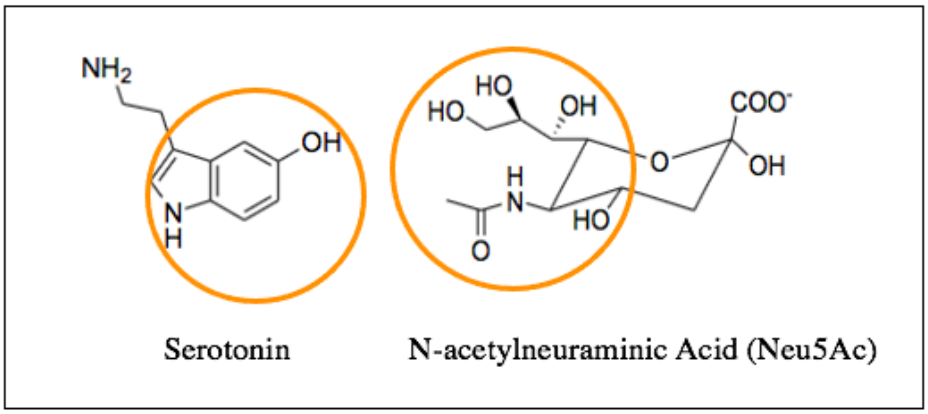


Figure 1.4. Binding sites between Serotonin and N-acetylneuraminic Acid

1.5 Aim of the Study

The aim was to develop a simple, sensitive, and selective colorimetric assay for determining N-acetylneuraminic acid and N-glycolylneuraminic sialic acid forms based on the plasmonic property of gold nanoparticles. Herein gold nanoparticles will be synthesized and functionalized with Serotonin. A UV-vis spectrophotometer

will be used to monitor a distinct color change from red to purple and blue due to the aggregation of modified particles in the presence of sialic acid. A systematic study of the response of gold nanoparticles to changes in sialic acid concentration in aqueous standards will be carried out. A series of factors affecting the assay and the synthesis of the Serotonin-gold nanoparticles will be carefully studied: amount and type of reactants, pH of the medium, reaction time for the chemical reactions, and recognition of sialic acid. Under optimized conditions, linearity, the calibration range and quantification limits (LOQs) of the plasmonic method will be found. Possible interference of the other sugars, including glucose, fructose, mannose, galactose, lactose, sucrose, and maltose, will be demonstrated. The method's potential for the accurate, sensitive, and convenient determination of sialic acids in biological samples will be presented. Figure 1.5 displays the schematic of the sialic acid assay investigated in this study.

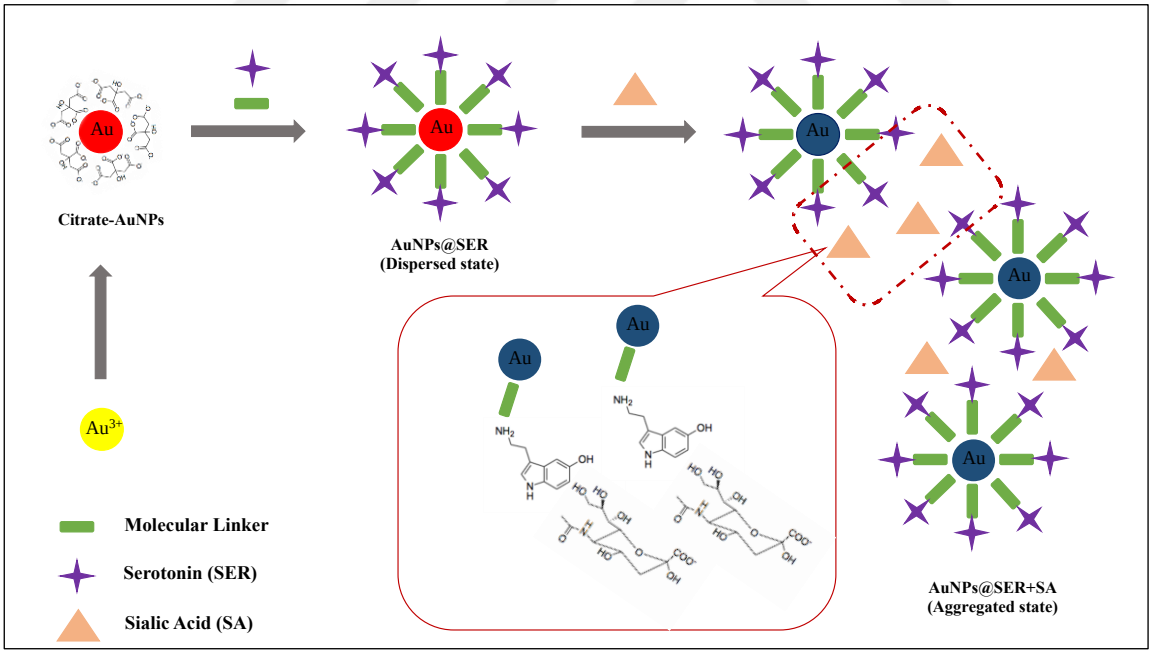


Figure 1.5. The schematic of sialic acid sensor

CHAPTER 2

EXPERIMENTAL

2.1 Chemicals and Reagents

18.2 M Ω.cm ultrapure deionized water was used for the preparation of all aqueous solutions. It was provided by ELGA LabWater, Purelab Option-Q water purification system.

2.1.1 Synthesis of Gold Nanoparticles

Sodium chloroaurate ($NaAuCl_4.2H_2O$, BDH) and sodium citrate tribasic dihydrate ($C_6H_5Na_3O_7.2H_2O$, ACS reagent, ≥ 99.0% Sigma- Aldrich) were used.

2.1.2 Serotonin Addition to Gold Nanoparticles via EDC/NHS Coupling

N-(3-Dimethylaminopropyl)-N'-ethylcarbodiimide hydrochloride (EDC.HCl, commercial grade, Sigma-Aldrich), N-Hydroxysuccinimide (NHS, >97%, Fluka), Serotonin hydrochloride (98%, Alfa Aesar) were used. Hydrochloric acid (HCl, ACS reagent, 37%, Sigma- Aldrich), sodium hydroxide (NaOH, puriss., 98-100.5%, pellets, Sigma-Aldrich), phosphoric acid (Fluka AG, Buchs SG, 84-85%) and potassium phosphate (98%, K_2HPO_4 Sigma-Aldrich) were used to adjust pH of EDC/NHS-AuNPs@SER solution.

2.1.3 Sialic Acid Determination using EDC/NHS-AuNPs@SER Probe

N-(-)-Acetylneuraminic acid (96%, abcr) and N-Glycolylneuraminic acid (BIOSYNTH Carbosynth) were used.

2.1.4 Functionalization of DSP onto Surface of Gold Nanoparticles

Dithiobis(succinimidylpropionate) (DSP, ProteoChem) and Sodium chloroaurate ($NaAuCl_4.2H_2O$, BDH) were used.

2.1.5 Serotonin and Sialic Acid Addition to DSP-AuNPs

Serotonin hydrochloride (98%, Alfa Aesar), N-(-)-Acetylneuraminic acid (96%, abcr) and N-Glycolylneuraminic acid (BIOSYNTH Carbosynth) were used. Hydrochloric acid (HCl, ACS reagent, 37%, Sigma- Aldrich), sodium hydroxide (NaOH, puriss., 98-100.5%, pellets, Sigma-Aldrich), phosphoric acid (Fluka AG, Buchs SG, 84-85%) and potassium phosphate (98%, K_2HPO_4 Sigma Aldrich) were used for change pH of DSP-AuNPs@SER solution.

2.1.6 Functionalization of DSP onto Surface of Gold Nanoparticles by Titration Method

Dithiobis(succinimidylpropionate) (DSP, ProteoChem) and Sodium chloroaurate ($NaAuCl_4.2H_2O$, BDH) were used.

2.1.7 Serotonin Addition to DSP-AuNPs

Serotonin hydrochloride (98%, Alfa Aesar) was used.

2.1.8 Sialic Acid Determination to AuNPs-DSP@SER probe

N-(-)-Acetylneuraminic acid (96%, abcr) and N-Glycolylneuraminic acid (BIOSYNTH Carbosynth) were used.

2.1.9 Selectivity Studies

D(+)-Glucose (anhydrous, reagent ACS), D(-)-Fructose (Fluka), D(+)-Mannose (99+%, ACROS ORGANICS), Lactose (Merck), Sucrose (99.5%, Sigma- Aldrich), D-(+)-Maltose monohydrate (BioUltra, ≥99.0%, Sigma- Aldrich) and N-(-)-Acetylneuraminic acid (96%, abcr) were used.

2.2 Instrumental

2.2.1 Ultrasonic Bath Sonicator

Elma Elmasonic S 40 Ultrasonic Bath was used to adjust temperature in all experiments.

2.2.2 Vortex Mixer

For the homogeneously preparation of all solutions, HEIDOLPH Reax Top VORTEX was used as a mixer.

2.2.3 Nutating Mixer

For gently shaking solution in order to get homogeneously dissolved solutions, VWR® Nutating Mixer was used.

2.2.4 pH Meter

For pH optimizations, PHM210 Standard pH Meter was used.

2.2.5 Centrifuge

For collecting gold nanoparticles by avoiding excess amount of EDC/NHS and Serotonin, NÜVE NF 200 Small Centrifuge was used.

2.2.6 Ultraviolet-Visible Spectrophotometry

The absorption spectra for colorimetric determination of sialic acid were collected by using a UV-Vis spectrophotometer. T80+ UV-VIS Instrument (PG Instruments Ltd.) with quartz cuvette and Multiskan Sky, Thermoscientific, USA Plate Reader were used.

2.2.7 Attenuated Total Reflection Fourier-Transform Infrared Spectrometer

For the identification of the formation of amide bond between Serotonin and DSP crosslinker, Bruker Alpha T ATR-FTIR was used.

2.2.8 Dynamic Light Scattering

For the determination size and surface potential of the synthesized AuNPs, Malvern Nano ZS90 was used.

2.2.9 Scanning Electron Microscopy

For the characterization of gold nanoparticles, QUANTA 400F Field Emission Scanning Electron Microscope located in METU Central Laboratory was used.

2.3 Procedures

2.3.1 Synthesis of Gold Nanoparticles

The synthesis of gold nanoparticles was followed by Turkevich Method [23]. Shortly, trisodium citrate dihydrate was added to boiling gold(III) chloride trihydrate solution with continuous stirring until the color of the solution became wine-red. To get more stable citrate stabilized gold nanoparticles, we optimized the mol ratio of trisodium citrate dihydrate ($Na_3C_6H_5O_7.2H_2O$) to sodium tetrachloroaurate dihydrate ($NaAuCl_4.2H_2O$) under different temperatures and different time intervals. Also, since the reaction pH was in the acidic region, we tried citric acid ($C_6H_8O_7$) rather than trisodium citrate dihydrate for pH studies.

To explain in more detail, 100 μL of 100 μM sodium tetrachloroaurate dihydrate was diluted to 20 mL with deionized water and boiled at under vigorous stirring. Then, 2.5 mL of 0.02 M trisodium citrate dihydrate was rapidly added. The mixed solution was boiled under stirring for 10 min. After being cool to room temperature, the resulting wine-red solution indicates the formation of citrate stabilized gold nanoparticles (AuNPs). It was stored in a refrigerator at 4^oC for further use.

UV-Vis spectrophotometer was used to follow the plasmonic absorption peak at 450-700 nm, the Dynamic Light Scattering (DLS) method to measure the average particle size, and Scanning Electron Microscope (SEM) to observe the shape and dispersity of gold nanoparticles.

2.3.2 Serotonin Addition to Gold Nanoparticles via EDC/NHS Coupling

The functionalization of EDC/NHS onto the surface of gold nanoparticles was based on a ligand exchange step [54]. The reason of the EDC/NHS functionalization is the modifying serotonin onto the gold nanoparticles. The optimum amount of EDC was determined experimentally, and equal moles of NHS with EDC was used. Therefore, the mole ratio of EDC/NHS in the solution was 1:1. Serotonin was added later. Serotonin concentration was used as twice the total concentration of EDC and NHS in the reaction mixture. To explain in more detail, 500 µL of 10.0 µM EDC and 10.0 µM NHS was added slowly to 10.0 mL citrate stabilized gold nanoparticles at room temperature under continuous stirring. Then, 500.0 µL of 20.0 µM Serotonin solution was added slowly. Subsequently, the solution was stirred for 2 hours at room temperature.

The resulting EDC/NHS-AuNPs@SER solution was subjected to centrifuging at optimized conditions (4000 rpm for 10 min) to eliminate the excess amount of EDC/NHS and SER. The circle was repeated several times until the supernatant solution became colorless. Afterward, the red EDC/NHS-AuNPs@SER sample at the bottom of the centrifuge tube was carefully collected and redispersed in DIW. The absorption spectrum was collected at 400-750 nm for characterization. The EDC/NHS-AuNPs@SER solution was stored at 4^{o}C when not in use.

2.3.3 Sialic Acid Determination to EDC/NHS-AuNPs@SER Probe

2.3.3.1 N-acetylneuraminic Acid Determination

Before adding N-acetylneuraminic acid, pH optimization of EDC/NHS-AuNPs@SER solution was performed using phosphate buffers at different pH values. 500.0 µL of different concentrations of N-acetylneuraminic acid (Neu5Ac) standard solutions were added to 500.0 µL of EDC/NHS-AuNPs@SER solutions to achieve final Neu5Ac concentrations of 5.0-750.0 µM in the final (total volume of

the solution was 1000 µL) solution. The absorption spectra of each mixture were measured at 400-800 nm after incubation for 5 minutes at room temperature.

The absorption spectra were collected every minute, over a total 15 min. A swift aggregation process that reaches saturation at about 10 min was observed. Hence, the incubation time was chosen as 5 min according to the results of absorbance ratio (A_{650}/A_{521}). Then, the absorption spectrum of each mixture was measured between 400 and 800 nm after incubation for 5 min at room temperature.

2.3.3.2 N-Glycolylneuraminic Acid Determination

500 µL of different concentrations of N-glycolylneuraminic acid (Neu5Gc) standard solutions were added to 500.0 µL of EDC/NHS-AuNPs@SER solutions to achieve final Neu5Ac concentrations of 5.0 -750.0 µM in the final (total volume of the solution was 1000 µL) solution. The absorption spectrum of each mixture was measured at 400-800 nm after incubation for 5 minutes at room temperature.

2.3.4 Functionalization of DSP onto AuNPs Surface

The functionalization of DSP onto the AuNPs surface was based on a ligand exchange step [31]. 20.0 µL of 2.0 mM DSP was added to 10.0 mL of synthesized AuNPs. Subsequently, the solution was stirred for 30 min at room temperature. Usually, centrifugation and a washing step are applied following a particle modification process to eliminate the excess reagents. However, we could not manage to redisperse DSP-AuNPs@SER particles after centrifugation. Therefore, the reaction solution was stored at 4^{o}C without any further treatment. For characterization of DSP-AuNPs, the absorption spectrum was measured between 400 and 800 nm.

2.3.5 Serotonin and N-acetylneuraminic Acid Addition to DSP-AuNPs

Since centrifugation could not be applied, we first added ligand Serotonin to the DSP-AuNPs solution to form Serotonin coated nanoparticles (AuNPs@SER) and then analyte sialic acid for the measurement.

A 10.0 mL of as-prepared AuNPs-DSP solution was diluted with 40.0 mL of 5.0 mM phosphate buffer (pH=5.6) [31]. A 1.25 mL of this colloidal solution was transferred to a 1.5 mL Eppendorf tube. The pH of the solution was adjusted using phosphate buffer or 0.1 M HCl or 0.1 M NaOH, and then, 0.125 mL of 6.0 μM serotonin was added. Subsequently, 0.125 mL of different concentrations of N-acetylneuraminic acid standard solutions were added to the DSP-AuNPs@SER solution to achieve final Neu5Ac concentrations of 1.7 -8.3 μM in the final solution.

The effect of reaction time was investigated by monitoring the aggregation in the presence of different concentrations of Neu5Ac by UV-Vis spectrophotometer. The absorption spectra were collected every minute, over a total ten minutes. A swift aggregation process that reaches saturation at about 5 min was observed. Hence, the incubation time was chosen as a one minute according to the results of absorbance ratio (A_{650}/A_{521}). Then, the absorption spectrum of each mixture was measured between 400 and 800 nm after incubation for 1 min at room temperature.

2.3.6 Optimization of the Amount of DSP to be used in the Surface Coating of AuNPs

To saturate the AuNPs surface with DSP, increasing volumes of 25.0 μM DSP were added to the diluted AuNPs solutions containing 0.150 mL of AuNPs [55]. The amounts of DSP used for titration are shown in Table 2.1. The total volume for each case was 1.5 mL. UV-vis spectrophotometer was used to measure the absorption spectra of the solutions between 250 and 300 nm.

Table 2.1. The Amounts of DSP used for titration

DSP (µL)	DSP (nmol)	DSP $_{final}$ (µM)
40	1.0	0.7
80	2.0	1.3
120	3.0	2.0
160	4.0	2.7
180	4.5	3.0
200	5.0	3.3
240	6.0	4.0

2.3.7 Optimization of the amount of Serotonin to be used in the surface coating of AuNPs

The optimum amount of DSP (2.7 µM; calculated from a titration) was added first to the diluted solution of AuNPs (150 µL in 940 µL phosphate buffer pH=5.6). Then, 125 µL of different Serotonin concentrations were added to the DSP-AuNPs solutions. The DSP:SER mol ratios in each aliquot are presented in Table 2.2. Each of these DSP-AuNPS@SER solutions was spiked with 125 µL of 100 µM N-acetylneuraminic acid. The absorbance spectra of the final solutions were measured between 400 and 800 nm.

The success of the ligand exchange reaction between citrate and DSP was investigated by ATR-FTIR measurement. Approximately 20.0 mL of DSP-AuNPs@SER solution was freeze-dried for ATR-FTIR measurements.

Table 2.2. DSP:SER mol ratio

DSP (nmol)	SER (nmol)	DSP:SER mol ratio
4.0	1.5	1 : 0.38
4.0	4.5	1 : 1.13
4.0	8.0	1 : 2.00
4.0	10.0	1 : 2.50
4.0	12.0	1 : 3.00
4.0	15.0	1 : 3.75

2.3.8 Sialic Acid Determination using DSP-AuNPs@SER Probe

2.3.8.1 N-acetylneuraminic Acid Determination

A 1250 µL of prepared DSP-AuNPs solution was transferred to a 1.5 mL Eppendorf tube, and then 125 µL of 6.7 µM Serotonin was added. Subsequently, 125 µL of different concentrations of sialic acid standard solutions were added to DSP-AuNPs@SER aliquots to achieve final Neu5Ac concentrations of 1.7 -58.3 µM in the final solution. The absorbance spectrum of each mixture was measured between 400 and 800 nm.

2.3.8.2 N-Glycolylneuraminic Acid Determination

A 1250 μL of prepared DSP-AuNPs solution was transferred to a 1.5 mL Eppendorf tube, and then 125 μL of 6.7 μM Serotonin was added. Subsequently, 125 μL of different concentrations of sialic acid standard solutions were added to DSP-AuNPs@SER aliquots to achieve final Neu5Gc concentrations of 1.7-58.3 μM in the final solution. The absorbance spectrum of each mixture was taken at 400-800 nm in one minute.

2.3.9 Selectivity

The selectivity of the present assay towards sialic acid was studied by comparing the response of both EDC/NHS-AuNPs@SER and DSP-AuNPs@SER under the influence of sugars including glucose, fructose, mannose, lactose, sucrose, and maltose. These sugars have similar cis-diols arrangements [31], so they can compete with sialic acid. The concentration of sugars selected as possible interferences was regulated ten times that of sialic acid.

2.3.9.1 Selectivity of EDC/NHS-AuNPs@SER probe towards Neu5Ac

The concentration of aqueous glucose, fructose, mannose, lactose, sucrose, and maltose solutions was 10.0 mM whereas, that of Neu5Ac was 0.1mM. Under this test, 500 μL of Neu5Ac and sugars were equally applied to 500 μL of EDC/NHS-AuNPs@SER aliquots. Moreover, the interfering effect of the mixture of all sugars were also studied. The absorption spectra of all aliquots were collected at 400-800 nm.

2.3.9.2 Selectivity of DSP-AuNPs@SER probe towards Neu5Ac

The concentration of aqueous glucose, fructose, mannose, lactose, sucrose, and maltose solutions was 10.0 mM whereas, that of Neu5Ac was 0.1mM. Assessing the effect of those sugars, 125 μL of 100 μM SA was first added into the 1375 μL of DSP-AuNPs aliquot to functionalize nanoparticles with serotonin, i.e., DSP-AuNPs@SER. After that, 500 μL of each sugar solution including Neu5Ac solution, were injected separately into the DSP-AuNPs@SER aliquots. Moreover, the interfering effect of the mixture of all sugars were also studied. The total volume of the reaction mixture in each case was 1500 μL. Then, their absorption spectra were collected at 400-800 nm. Separation of N-acetylneuraminic acid and N-glycolylneuraminic acid from their mixture.

CHAPTER 3

RESULTS AND DISCUSSION

3.1 Synthesis of Gold Nanoparticles

Gold nanoparticles were synthesized using the sodium citrate reduction method [23]. Parameters such as mole ratios of reactants, reaction temperature, and time were optimized. We started by using trisodium citrate dihydrate and sodium tetrachloroaurate dihydrate in three different molar ratios to evaluate the change in stability and absorption properties of gold nanoparticle solutions. Table 3.1 presents the mole ratios of Au^{3+}/citrate.

Table 3.1 Mole ratios of Au^{3+}/Citrate in gold nanoparticle solutions

Solution number	**Citrate (mol)**	**Au^{3+} (mol)**	**Mol ratio of Citrate/Au^{3+}**
1	2.55×10^{-4}	1.0×10^{-5}	25.5
2	1.70×10^{-4}	1.0×10^{-5}	17.0
3	1.02×10^{-4}	1.0×10^{-5}	10.2

The maximum absorption wavelengths and intensities of solutions number 1 and 2 are somewhat similar. It indicates that there is not much difference in their plasmonic

properties. However, the shelf life of solution-2 was longer than others. Therefore, it was decided to continue with solution 2 due to its better stability.

The effect of temperature was investigated by synthesizing the gold nanoparticles at 80, 85, and 90 °C. Additionally, the duration of the synthesis reaction was also varied. The summary of the parameters used in temperature and time optimization of gold nanoparticle synthesis, where the mol ratio of citrate/Au^{3+} is 17.0. The colors of nanoparticle solutions are also presented in the Table 3.2.

Table 3.2 Parameters used in temperature and time optimizations of citrate stabilized gold nanoparticle synthesis

Solution number	Temperature (°C)	Time (min)	Color
1	90	10	
2	85	25	
3	80	5	
4	80	10	
5	80	15	
6	80	60	

As seen in the first two rows of Table 3.2, when the reaction temperatures are 85 and 90°C, the color of the solutions is red. If the reaction temperature is 80°C, no color change in the solution is observed even if the duration is extended to 60 minutes. In

addition to the visual color monitoring, their UV-Vis absorption spectra were also measured between 450 and 700 nm, Figure 3.1.

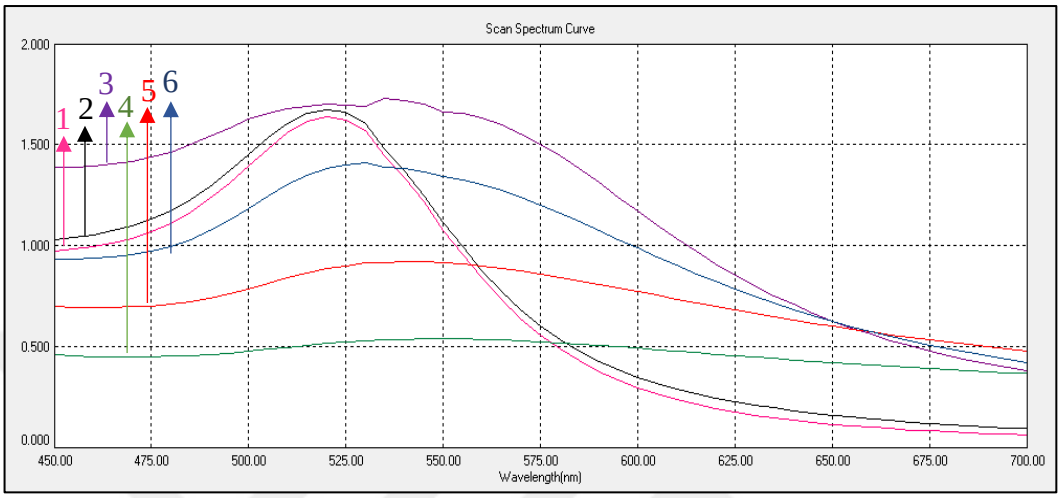


Figure 3.1 The absorption spectra of citrate stabilized gold nanoparticles at different temperatures and times. 1 to 6 refers to solution numbers given in Table 3.2

Spectra of solutions 1 and 2 show characteristic well-defined absorption peaks at 521 nm with relatively narrow half bandwidth, whereas the absorption spectra of others (Sample numbers 3-6) are broad. We can conclude that gold nanoparticle formation occurred at 85^{o}C and 90^{o}C; however, the complete reduction did not happen at 80^{o}C at the specified conditions. 90^{o}C is selected as reaction temperature due to its short duration time.

Sodium citrate is frequently used to synthesize gold nanoparticles due to its cheapness and nontoxicity. It acts both as the reducing and the charge stabilizing agents of the AuNPs [56]. Trisodium citrate dihydrate is a conjugate base of citric acid. We decided to use its acidic form to study pH, citric acid ($C_6H_8O_7$), for nanoparticle synthesis under specific conditions given in Table 3.3. Briefly, citric acid was added to boiling sodium tetrachloroauratedihydrate solution under continuous stirring for 15 min. However, the characteristic ruby color could not be

observed (Table 3.3). Thus, we concluded that citric acid could not be used for the synthesis of gold nanoparticles for our procedure.

Table 3.3 Temperature optimization of gold nanoparticle synthesis by using 1.575 x 10^{-6} mol of citric acid

Solution number	Au^{3+}	Mol ratio of Citric acid/Au^{3+}	Temperature (^oC)	Color
1	2.10 x 10^{-6}	0.75	50	
2	2.10 x 10^{-6}	0.75	80	
3	1.05 x 10^{-6}	1.50	50	
4	1.05 x 10^{-6}	1.50	80	
5	5.25 x 10^{-7}	3.00	80	

Optimum condition for the synthesis of gold nanoparticles was found after those optimizations. Shortly, trisodium citrate dihydrate was added to boiling gold(III) chloride trihydrate solution at 90^{o}C with continuous stirring until the color of the solution became wine-red as shown in Figure 3.2.



Figure 3.2 The red color of gold nanoparticles

It has been stated that [57] the chemical environment is very determinative for citrate binding. The alteration of pH, cations, and anions may have caused the failure in nanoparticle synthesis. Therefore, the particles were traditionally synthesized using trisodium citrate dihydrate [58].

According to the Dynamic Light Scattering (DLS) measurements, the synthesized citrate stabilized gold nanoparticles have an average particle size of 20.35 ± 0.67 nm. The size distribution graph is given in Figure 3.3. The molar concentration of nanoparticle can be determined by its average particle size [59]. From its average particle size, concentration of synthesized gold nanoparticles was calculated as 3.5 nM.

The experimental extinction coefficient of gold nanoparticles was determined according to Lambert–Beer law [59] , and it was calculated as 1.46×10^9 $M^{-1}cm^{-1}$. Shortly, the gold nanoparticle solution was diluted into solutions into different concentrations. The absorption spectrum of each solution at 521 nm was measured. The absorbance at 521 nm versus the molar concentration of the solution graph was plotted. The extinction coefficient was the slope of the curve.

From its average particle size, the theoretical extinction coefficient was found as 1.09×10^9 $M^{-1}cm^{-1}$ by using the extinction coefficients table of gold nanoparticles with different core sizes [59]. There is no significant difference between experimental and theoretical extinction coefficients.

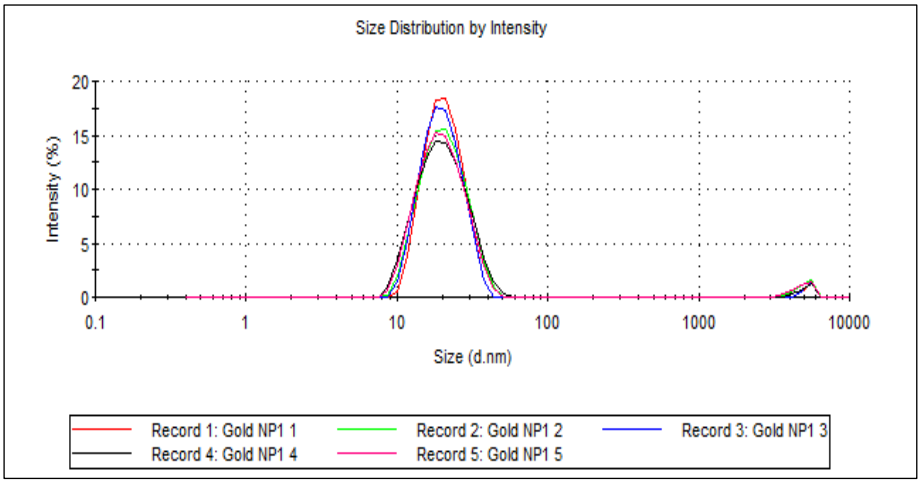


Figure 3.3. Size Distribution graph of gold nanoparticles

Scanning electron microscope images of AuNPs were shown in Figure 3.4. The SEM images reveal that gold nanoparticles are spherical and dispersed. The EDX spectrum showed that the detected particles correspond to gold, as shown in Figure 3.5.

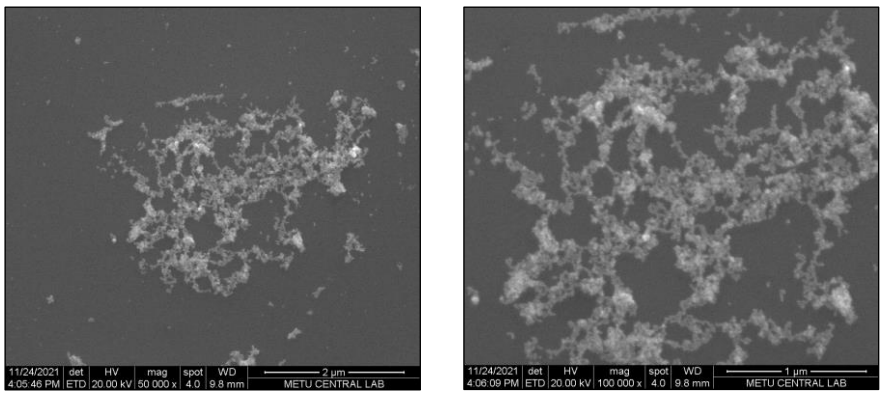


Figure 3.4. SEM images of gold nanoparticles

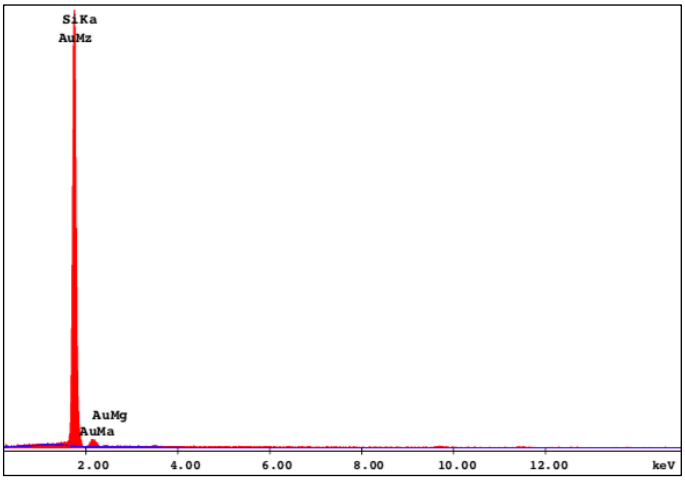


Figure 3.5. EDX analysis of AuNPs formed by reduction of sodium tetrachloroaurate dihydrate by trisodium citrate dihydrate

3.2 Serotonin Addition to AuNPs via EDC/NHS Coupling

The possible binding sites of Serotonin and N-acetylneuraminic acid are shown in Figure 1.4. Amine group of the serotonin does not play an active role in the affinity interaction with sialic acid. Therefore, it was decided to prepare the AuNPs@SER nanoparticles through a standard [60] three-step amine coupling reaction, which includes an EDC/NHS chemistry, as shown in Figure 3.6. Surface modification process and washing steps often give rise to problems due to the aggregation of the particles. Therefore, we optimized the amount of the reagents and centrifugation conditions in the adapted method as mentioned in experimental part.

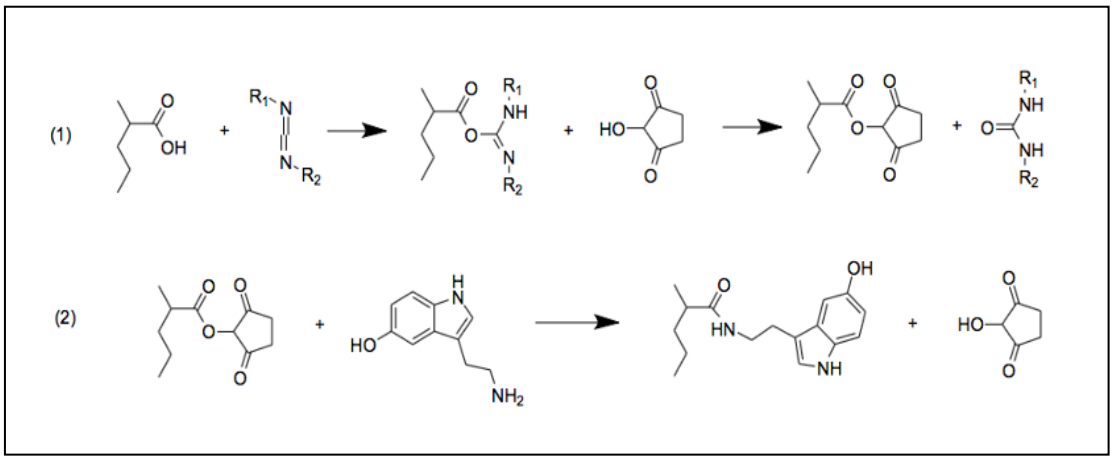


Figure 3.6 The chemical reaction scheme for the amine coupling. The carboxyl group is activated with EDC/NHS (1) followed by covalent attachment of Serotonin by its primary amine (2)

The absorption spectrum of EDC/NHS-AuNPs@SER was collected by a UV-Vis spectrophotometer, which is shown in Figure 3.7. First of all, Neu5Ac was added to EDC/NHS-AuNPs in the absence of Serotonin. The new peak was not observed as seen in Figure 3.7 (a). That means that EDC/NHS-AuNPs cannot be used for sialic acid determination. However, when Neu5Ac was added to EDC/NHS-AuNPs@SER, the new peak was observed as seen in Figure 3.7 (b).

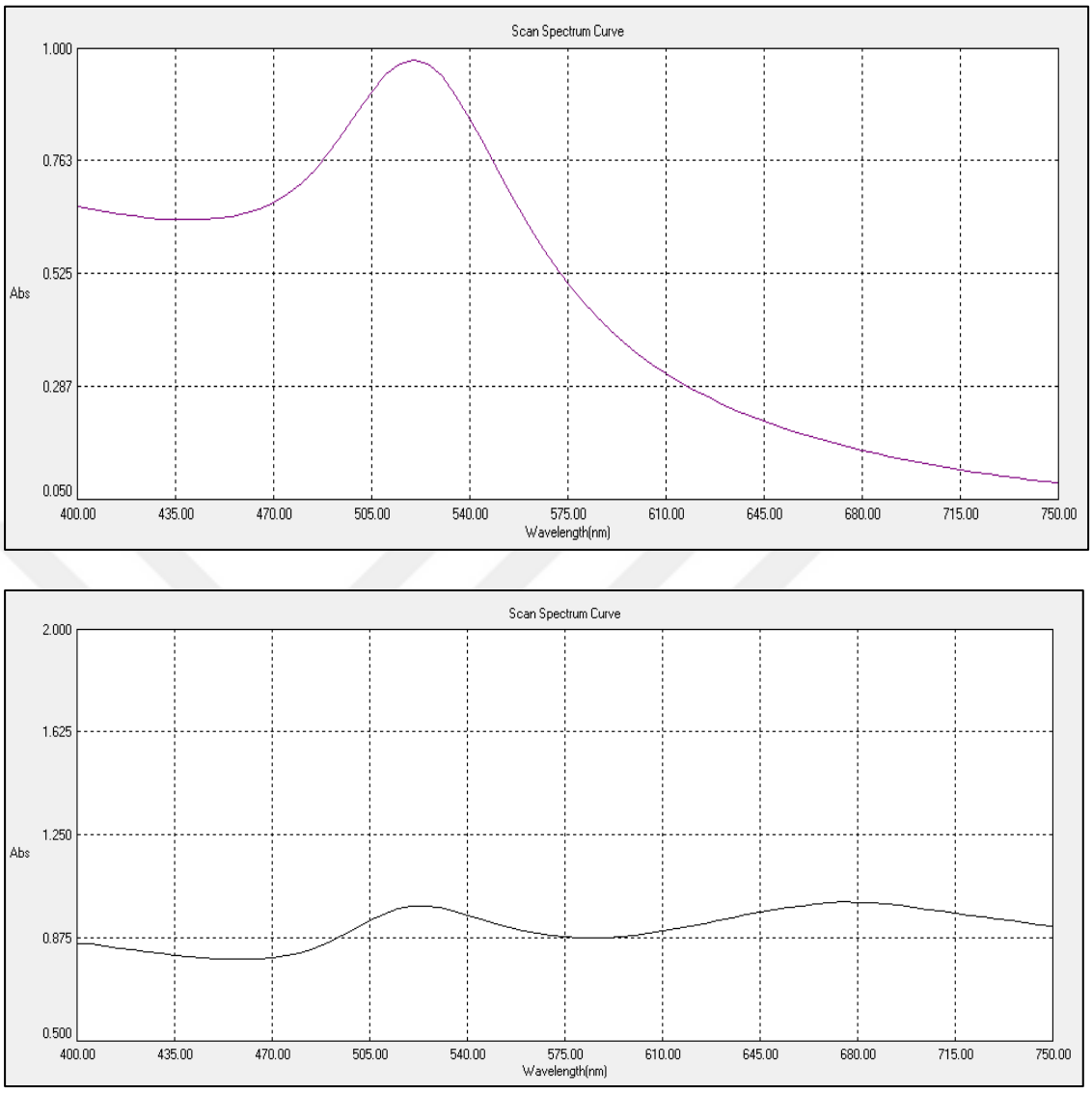


Figure 3.7 Absorption spectra of Neu5Ac addition to (a) EDC/NHS-AuNPs and (b) EDC/NHS-AuNPs@SER

3.3 Sialic Acid Determination using EDC/NHS-AuNPs@SER Probe

In this section, we investigated the performance of the probe in the detection of Neu5Ac and Neu5Gc sialic acids. Parameters such as pH, time, and temperature were optimized to lower the detection limit for the analysis. Among them, pH affects

the surface charge of nanoparticles and can cause particles to behave differently in acidic and alkaline conditions. As we mentioned earlier, the stability of nanoparticle solutions in the absence of the analyte is essential for sensor applications. Therefore, the stability of EDC/NHS-AuNPs@SER probes was tested at diverse pH values. The ruby color of the solutions turning purple or blue was considered as destabilization of the particles due to aggregate formation.

As a result, EDC/NHS-AuNPs@SER solutions with pH values of 2.3, 5.4, 7.4 and 10.0 were prepared using 10.0 mM phosphate buffer. The colors of EDC/NHS-AuNPs@SER solutions at these pH values are presented in Figure 3.8 with the same pH order.



Figure 3.8 The color of EDC/NHS-AuNPs@SER at pH from left to right 2.3, 5.4, 7.4 and 10.0, respectively

Solution's ruby color at pH 2.3 and 10.0 was turned purple and light blue, respectively, whereas, at pH 5.4 and 7.4, no color change was observed, as shown in Figure 3.10. Therefore, it was concluded that the pH in the 5.0-8.0 range is suitable for sensor application.

3.3.1 Neu5Ac Determination using EDC/NHS-AuNPs@SER Probe

Neu5Ac is an analyte; purple to the blue color transformation of the probe aliquots was expected following its addition due to the affinity interaction with nanoparticles.

1.0 mL of 1.0 mM N-acetylneuraminic acid was added to each 1 mL of EDC/NHS-AuNPs@SER solution at pH 5.4 and 7.4. The colors of solutions before and immediately after Neu5Ac addition are shown in Figure 3.9.



Figure 3.9 The color of EDC/NHS-AuNPs@SER solutions at pH from left to right 5.4 in the absence of Neu5Ac, at pH 5.4 in the presence of Neu5Ac, at pH 7.4 in the absence of Neu5Ac, at pH 7.4 in the presence of Neu5Ac, respectively. Reaction time was 5 min

After 15 min, however, we observed a color change to purple in the EDC/NHS-AuNPs@SER aliquot spiked with Neu5Ac at pH 5.4, whereas there was no color change at pH 7.4. We thoroughly examined the 5.0 -7.4 pH region for the probe's reactivity and found that the pH 5.0-7.0 region was suitable for the measurements.

Since the pH of the EDC/NHS-AuNPs@SER solution was 6.5, we did not make any pH adjustment before the analyte addition. The color change of the EDC/NHS-AuNPs@SER probe at Neu5Ac concentrations of 5.0 to 750.0 μM is shown in Figure 3.10. According to the figure, a corresponding color transition from ruby red to purple and finally, blue and gray was observed, which indicates the change of dispersion to aggregation state accordingly to the concentrations of SA.

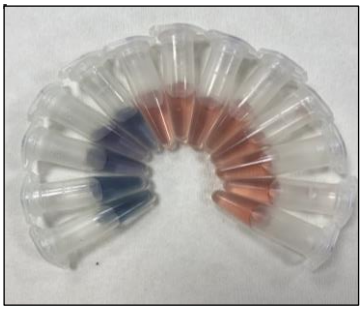


Figure 3.10 Color scheme of EDC/NHS-AuNPs@SER after addition from 5 to 750 μM of Neu5Ac standard solutions, respectively

The absorption spectra of the EDC/NHS-AuNPs@SER probe in Neu5Ac solutions having concentrations of 5 to 750 μM, are shown in Figure 3.11. The presence of only the absorption peak of gold nanoparticles in the spectra indicates that the EDC/NHS-AuNPs@SER probe could not respond to Neu5Ac concentrations below 300 μM.

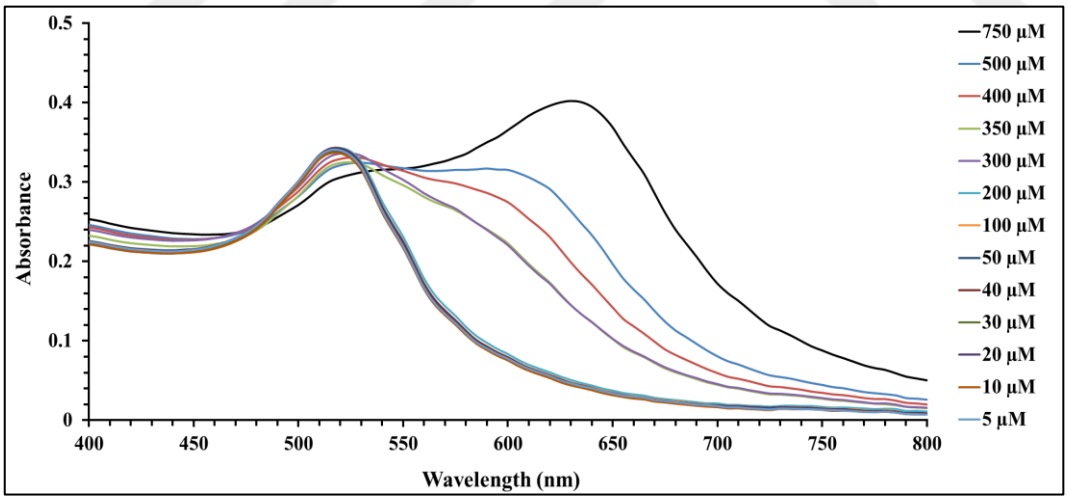


Figure 3.11 Red shift in the absorbance spectrum of EDC/NHS-AuNPs@SER probes in 5 to 750 μM of Neu5Ac standard solutions, respectively

In the 300.0 and 750.0 µM concentration range, the absorbance measured at 521 and 625 nm wavelengths were used to calculate the absorbance ratio of A_{625}/A_{521}. A_{625}/A_{521} versus Neu5Ac concentration (µM) plot is shown in Figure 3.12.

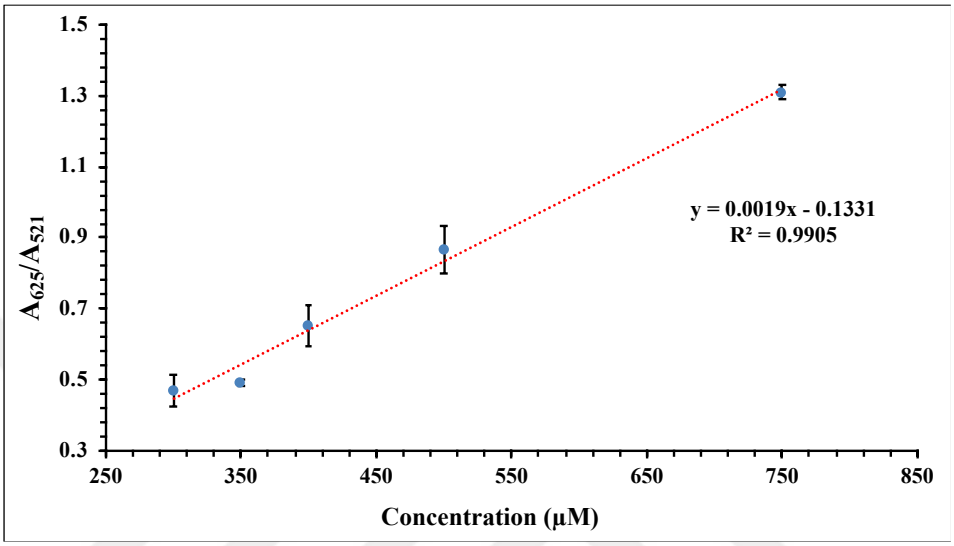


Figure 3.12 Calibration plot obtained after addition of Neu5Ac

Line equation, R-squared (R^2), limit of quantification (LOQ) and linear dynamic range (LDR) values derived from the calibration plot, are summarized in Table 3.4. LOQ value was calculated as 257.5 µM, based on 10 δ/m where δ is the standard deviation of the blank and m is the slope of the calibration curve [31]. EDC/NHS-AuNPs@SER probe can be used successfully for the determination of Neu5Ac above 257.5 µM levels.

Table 3.4. The statistical data obtained from calibration plot in Figure 3.12

Calibration curve equation	**R^2**	**LOQ (µM)**	**LDR (µM)**
y=0.0019x-0.1331	0.9905	257.5	257.5-750.0

3.3.2 Neu5Gc Determination using EDC/NHS-AuNPs@SER Probe

N-glycolylneuraminic acid (Neu5Gc) was added to EDC/NHS-AuNPs@SER probe rather than N-acetylneuraminic acid (Neu5Ac). Although only the methyl group of Neu5Ac' acetyl group is being replaced with OH, the affinity of the serotonin to Neu5Gc changes significantly [61]. The concentration ranges from 5 to 500 µM that has been used in the Neu5Ac determination was also applied for the determination of Neu5Gc. The behavior of the probe however was quite different. The colors of EDC/NHS-AuNPs@SER probe in the presence of various Neu5Gc concentrations and their absorption spectra are shown in Figure 3.13, and Figure 3.14 respectively.



Figure 3.13 The color change of EDC/NHS-AuNPs@SER probes in 5 to 500µM of Neu5Gc standard solutions, respectively

The range of concentration investigated was 5.0 to 500.0 µM. The presence of only the absorption peak of gold nanoparticles in the spectra (Fig. 3.14) indicates that the EDC/NHS-AuNPs@SER probe does not interact with Neu5Gc even at the highest concentration.

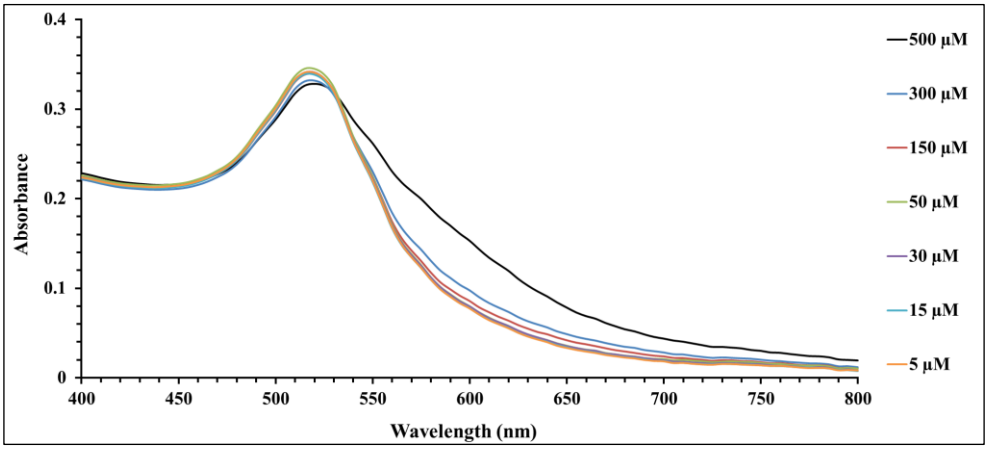


Figure 3.14 EDC/NHS-AuNPs@SER probes in 5 to 500 µM of Neu5Gc standard solutions, respectively

3.4 The Functionalization of DSP on the AuNPs Surface

DSP crosslinker was chosen to functionalize gold nanoparticles [31]. The DSP crosslinker increases the stability of gold nanoparticles by replacing weak citrate bonds with a firm Au-S covalent bond. Besides, it provides easy attachment of Serotonin to the surface with the succinimidyl propionate groups in its structure.

Figure 3.15 shows the absorbance spectrum of DSP stabilized gold nanoparticles. We see no change when comparing the absorbance spectrum of nanoparticles stabilized with citrate.

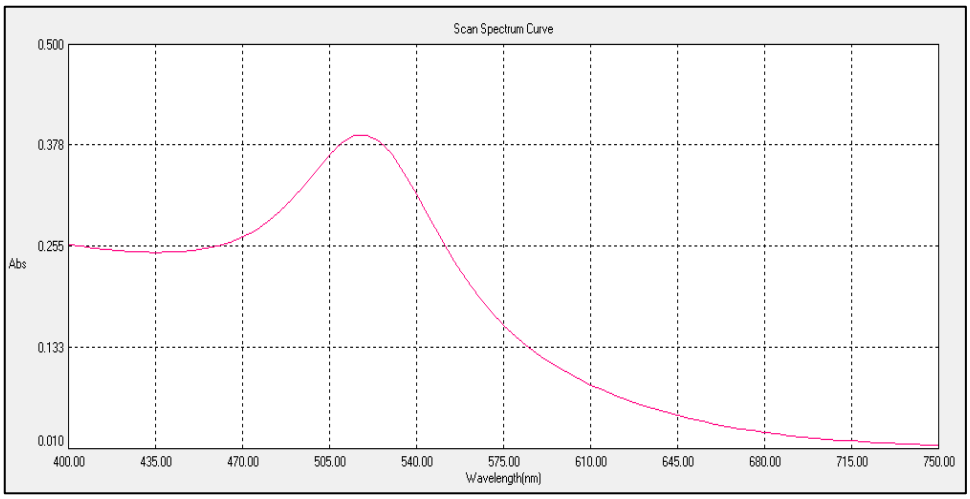


Figure 3.15 The absorption spectrum of DSP-AuNPs

3.5 Serotonin Addition to DSP-AuNPs and Neu5Ac Determination using DSP-AuNPs@SER Probe

DSP can provide serotonin assembling due to the amide bond between DSP and serotonin [31]. The other side of serotonin is exposed to the solution for N-acetylneuraminic acid-binding.

The original pH value of the DSP-AuNPs@SER was 6.42. N-acetylneuraminic acid having a pH of 1.1 can alter the pH of the DSP-AuNPs@SER solution in their mixtures. Thus, before adding N-acetylneuraminic acid, the stability of the DSP-AuNPs@SER solutions was tested at various pH values. A set of solutions containing DSP-AuNPs@SER probes at pH values of 2.0; 3.0; 4.0; 9.0 and, 11.0 were prepared. The colors of the solutions are given in Figure 3.16.

In the acidic region, pH<4.0, the aliquot's color was blue due to the aggregation, shown in Figure 3.16. At pH values above 4.0, on the other hand, the original red color of the solutions is preserved. As a result, any pH above 4.0 can be safely used for sensor applications. As pH of the solution increases, the time required for sialic acid determination is increases accordingly.



Figure 3.16 The color of DSP-AuNPs@SER at pH from left to right 2.0, 3.0, 4.0, 9.0, and 11.0, respectively

In the original DSP-gold nanoparticle preparation protocol [31], the pH was 5.4. Therefore, we also decided to use the same pH in our studies. Different concentrations of N-acetylneuraminic acid were added to DSP-AuNPs@SER solutions. N-acetylneuraminic acid concentrations of the aliquots are shown in Table 3.5. Their absorption spectra are given in Figure 3.17. The last row of Table 3.5 corresponds to a phosphate buffer at pH 5.6, having DSP-AuNPs@SER probes solely.

Table 3.5 The final concentrations of N-acetylneuraminic acid

Solution number	**Neu5Ac (µM)**
1	8.3
2	6.7
3	5.0
4	3.3
5	1.7
6	0

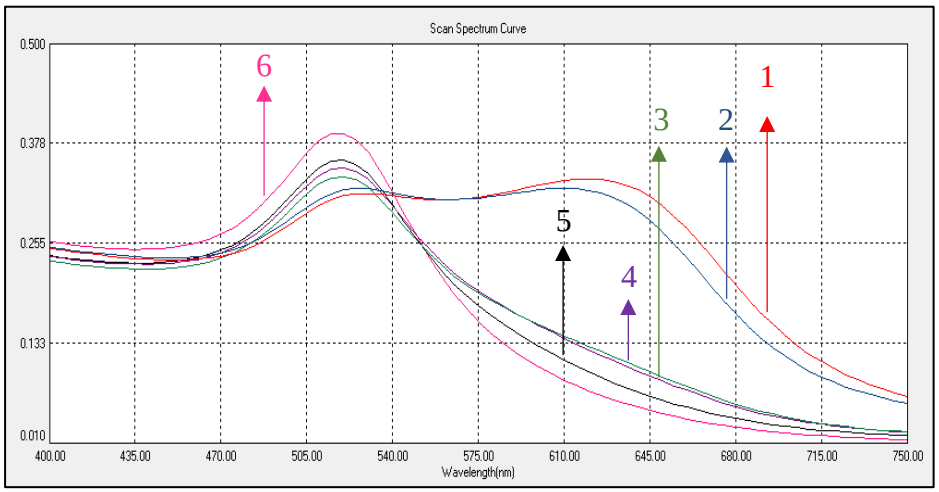


Figure 3.17 The absorption spectra of DSP-AuNPs@SER and DSP-AuNPs@SER probes in various concentrations of Neu5Ac standard solutions. 1 to 6 refers to solution numbers given in Table 3.5

The spectrum of solution number 6 shows the original peak position of DSP-AuNPs@SER probe at 521 nm. The spectra of the solution number 5 to 3 are similar to the DSP-AuNPs@SER probe's spectrum. At Neu5Ac concentrations 6.7 and 8.3 µM, the second peaks at 625 nm have emerged clearly. The same measurements were repeated three times on different days, but the absorption spectra did not change.

As mentioned in the experimental section, it was impossible to centrifuge these solutions to collect the particles. Therefore, we decided to find the minimum DSP and serotonin amounts necessary to prepare DSP-AuNPs@SER probes. So, two titration reactions were carried out, as explained in the following sections.

3.6 Optimization of the Amount of DSP to be used in the Surface Coating of AuNPs

It has been reported that the gold nanoparticle solution was titrated with DSP to find the optimum amount of DSP for coating the surfaces of gold nanoparticles [55]. It is stated that when DSP is bonded to the gold surface, the accessibility of water ions to the propionate carbonyl of DSP is restricted, thus reducing the hydrolysis process.

The hydrolyzed form of the succinimidyl group gives an absorption spectrum at λ_{max} of 260 nm. It is possible to follow the rate of hydrolysis by monitoring the change in absorbance at 260 nm. Therefore, photometric titration of gold nanoparticle solution with DSP will be performed. If there is a gold surface on which the DSP can be adsorbed, there will be a slight variation in the measured absorbance values. If the gold surface is saturated with DSP, excess DSP will remain in the solution, and a linear increase in absorbance values will be observed in parallel with the increasing amount of DSP. The DSP concentration at which this rapid increase begins will be considered the saturation concentration**.**

A diluted solution containing 150 µL of AuNPs was titrated with DSP [50]. The volumes, number of moles of DSP solution, and the final concentrations of DSP are given in Table 3.6. Absorbance values at 260 nm were measured right after and 1 min after each DSP addition. The ΔA_{260}/min versus DSP (nmol) graph was plotted, as shown in Figure 3.18.

Table 3.6 The volumes and number of nmoles of titrant and DSP concentrations in the final aqueous solution containing 150 µL of AuNPs

DSP (µL)	**DSP (nmol)**	**DSP $_{final}$ (µM)**
40	1.0	0.7
80	2.0	1.3
120	3.0	2.0
160	4.0	2.7
180	4.5	3.0
200	5.0	3.3
240	6.0	4.0

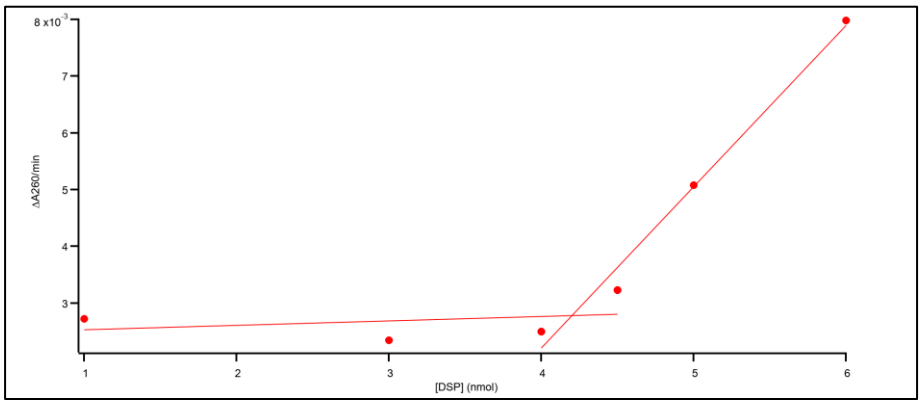


Figure 3.18 Photometric titration curve: The rate of DSP hydrolysis was monitored at 260 nm following the additions of DSP standard solution to DIW containing 150 µL of AuNPs

The end point of the titration is at 4.1 nmol DSP . At that point, gold nanoparticles should be saturated with DSP. Higher amounts of 4.1 nmol DSP will be excess in the solution. To be safe, we decided to add 4.1 nmol DSP to the solution containing 150 µL of AuNPs, which led to 2.7 µM DSP.

3.7 Optimization of the Amount of Serotonin to be used in the Surface Coating of AuNPs

The stoichiometric ratio of DSP: SER is 1:2 [31]. However, this ratio may change after surface modification of gold nanoparticles with DSP. Therefore, various DSP: SER mole ratios, Table 3.7, were used for surface modification of the DSP-AuNPs. The same amount of Neu5Ac was added to each of these solutions. The eye inspected the color of the solutions, and their absorbance spectra were taken, as shown in Figure 3.19.

Table 3.7 Mol ratio of DSP:SER

Solution number	DSP (nmol)	SER (nmol)	Mol ratio of DSP:SER
1	4.0	1.5	1 : 0.38
2	4.0	4.5	1 : 1.13
3	4.0	8.0	1 : 2.00
4	4.0	10.0	1 : 2.50
5	4.0	12.0	1 : 3.00
6	4.0	15.0	1 : 3.75

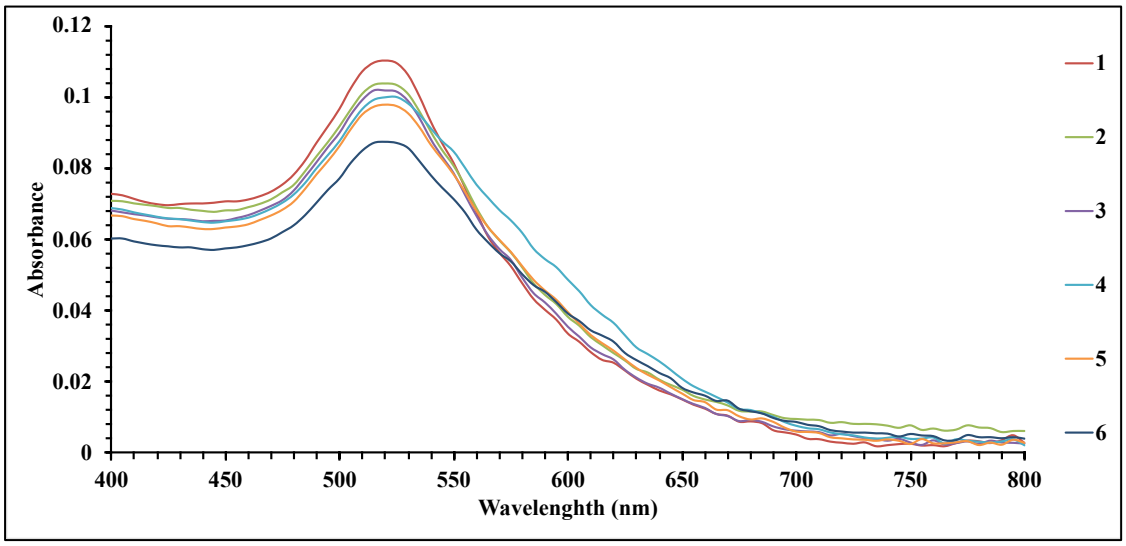


Figure 3.19 The absorption spectra after Neu5Ac addition to DSP-AuNPs@SER with different SER concentrations

The color of the solution 4 changed from purple upon addition to Neu5Ac. Then, Solution 5 and 6 changed color to blue in 2 minutes. Solution 1, 2 and 3 were changed color after 5 minutes. The minimum amount of Serotonin should be used due to the agglomeration in centrifuge step. The excess amount of Serotonin cannot be modified on gold nanoparticle surface. Time was another important parameter. Thus, Solution 4 (the mol ratio of DSP:SER equals to 1:2.50) was chosen for the determination of sialic acid.

The FTIR measurements were done to investigate the functional groups on the surface (Figure 3.20). The surface of the gold nanoparticles was initially coated with citrate. Characteristic citrate peaks were reported at 1395 and 1586 cm^{-1} [62]. The gold nanoparticles were then modified by DSP. The reported peaks of DSP were 1710.6 cm^{-1} (CO stretch), 1421.7 and 1363.2 cm^{-1} (C-H bending vibrations of methylene), and 1235.3 and 1095.0 cm^{-1} (asymmetric and symmetrical C-O stretching vibrations) [63]. The last modification was done with Serotonin. Characteristic peaks of which were 1466, 1376, and 1513cm^{-1} (Aromatic C-C extensions), 1206 cm^{-1} (in-plane bending of the aromatic C-H bond) [64]. The spectra of DSP-AuNPs@SER is shown in Figure 3.19.

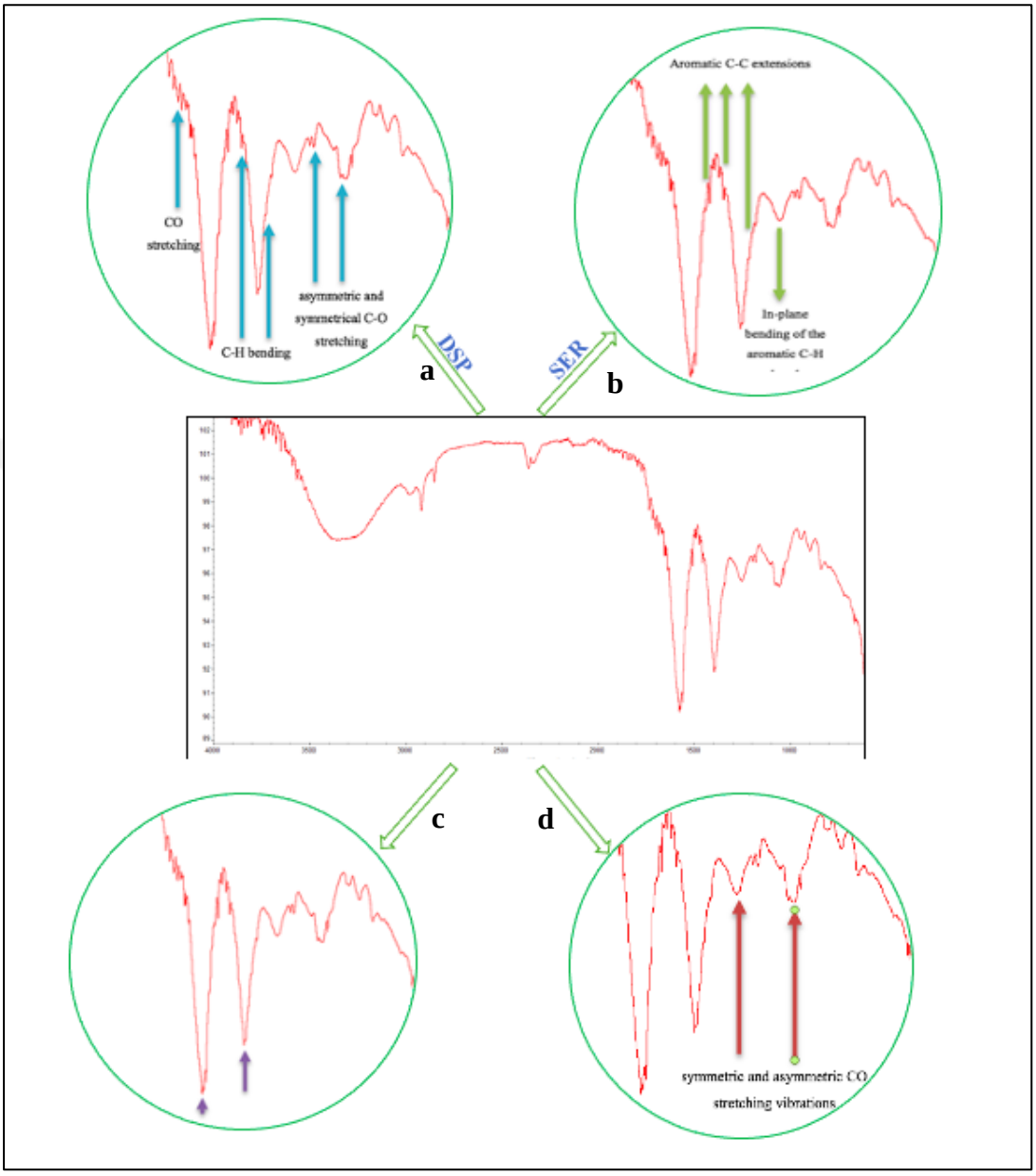


Figure 3.20 ATR-FTIR spectrum of DSP-AuNPs (a) expected peaks of DSP (b) expected peaks of SER (c) observed prominent peaks of DSP-AuNPs@SER (d) observed CO stretching belongs to DSP

As can be seen from the spectrum, the prominent peaks of DSP-AuNPs@SER nanoparticles are at 1586 and 1395 cm^{-1}. These peaks are thought to belong to the citrate groups that remained unchanged on the surface. These two broad peaks are probably masking the CO stretching, and CH bending vibrations of DSP and the aromatic ring CC stretches of Serotonin. On the other hand, observing the symmetric ($1095cm^{-1}$) and asymmetric ($1238cm^{-1}$) vibrations of the CO stretching is thought to indicate the presence of DSP on the surface.

3.8 Sialic Acid Determination using DSP-AuNPs@SER Probe

In this section, we investigated the performance of the DSP-AuNPs@SER probe in the detection of Neu5Ac and Neu5Gc sialic acids. Parameters such as pH, time and temperature were optimized, as we mentioned earlier, to achieve the lowest possible detection limits for the determination of sialic acid.

3.8.1 Neu5Ac Determination using DSP-AuNPs@SER Probe

Different concentrations of Neu5Ac were added to DSP-AuNPs@SER solution. Then, the absorption spectra were collected, as shown in Figure 3.21. Figure 3.22 shows the color of DSP-AuNPs@SER solutions immediately after Neu5Ac addition.

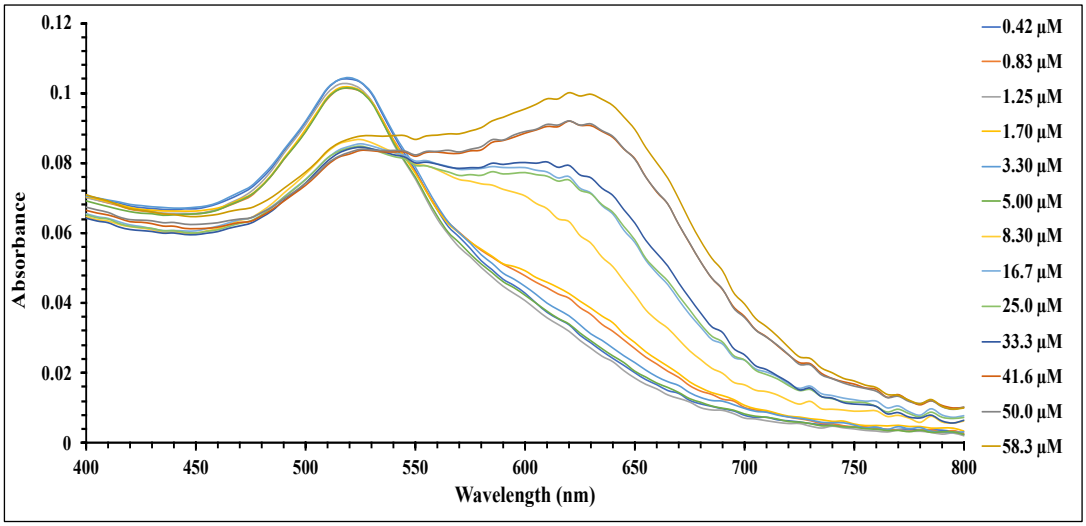


Figure 3.21 Absorbance spectra of DSP-AuNPs@SER probe in (0.42 to 58.3 µM) concentration of Neu5Ac solutions



Figure 3.22 DSP-AuNPs@SER nanoparticles in 58.3, 50.0, 41.6, 33.0, 25.0, 16.7 and 8.30 µM Neu5Ac, respectively

In the 8.30 and 58.30 µM concentration range, the absorbencies measured at 521 and 625 nm wavelengths were used to calculate the absorbance ratio. A_{625}/A_{521} versus Neu5Ac concentration (µM) plot is shown in Figure 3.23.

.

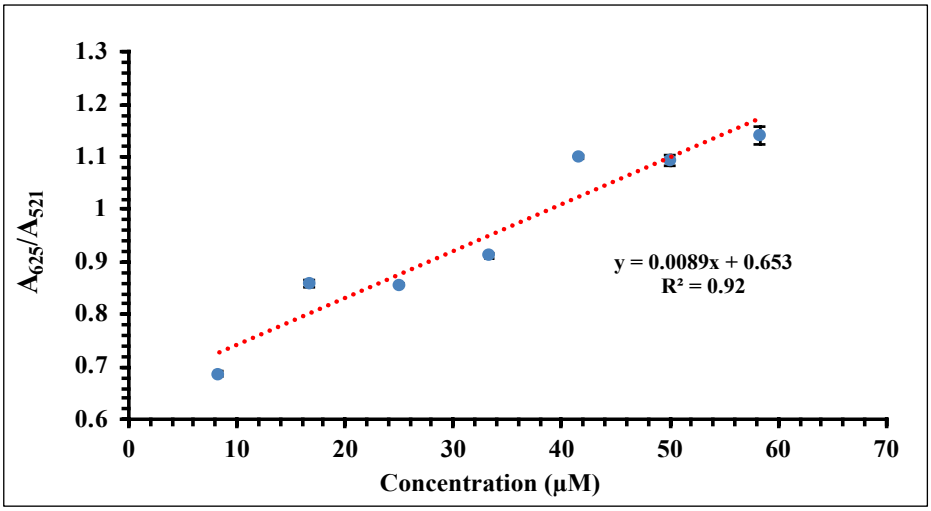


Figure 3.23 Calibration plot for Neu5Ac measurements

Line equation, R-squared (R^2), limit of quantification (LOQ) and linear dynamic range (LDR) values derived from the calibration plot, are summarized in Table 3.8. LOQ value was calculated as µM, based on 10 δ/m where δ is the standard deviation of the blank and m is the slope of the calibration curve [31]. DSP-AuNPs@SER probe can be used successfully for the determination of Neu5Ac above 10.0 µM levels.

Table 3.8. The statistical data obtained from calibration plot in Figure 3.23

Calibration curve equation	**R^2**	**LOQ (µM)**	**LDR (µM)**
y=0.0089x+0.653	0.92	10.0	10.0 -58.3

3.8.2 Neu5Gc Determination using DSP-AuNPs@SER Probe

N-glycolylneuraminic acid was added to DSP-AuNPs@SER probe rather than N-acetylneuraminic acid. Although only the methyl group of Neu5Ac' acetyl group is being replaced with OH, the affinity of the Serotonin to Neu5Gc changes significantly [58]. The concentration ranges from 1.70 to 58.30 µM that has been used in the Neu5Ac determination was also used for the determination of Neu5Gc. The absorption spectra of DSP-AuNPs@SER probe in the presence of various Neu5Gc concentrations are shown in Figure 3.24.

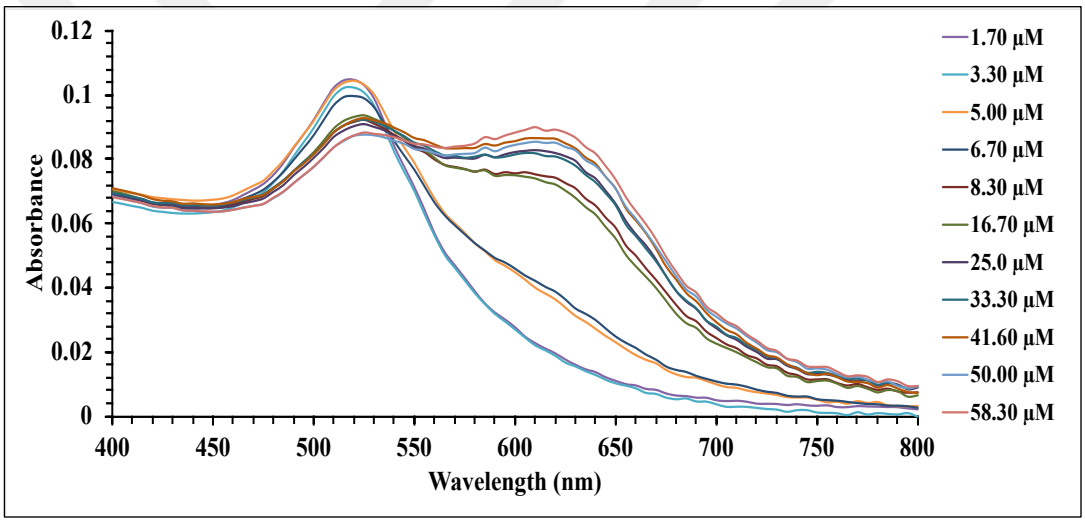


Figure 3.24 Absorbance spectra of DSP-AuNPs@SER probes in (1.70 to 58.3 µM) concentration of Neu5Gc solutions

In the 16.70 and 58.30 µM concentration range, the absorbances measured at 521 and 625 nm wavelengths were used to calculate the absorbance ratio. A_{625}/A_{521} versus Neu5Gc concentration (µM) plot is shown in Figure 3.25.

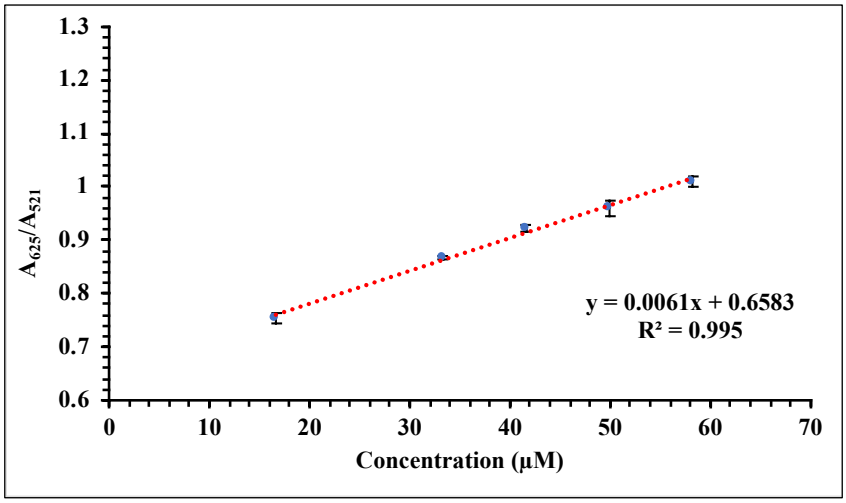


Figure 3.25 Calibration plot obtained after addition of Neu5Gc

Line equation, R-squared (R^2), limit of quantification (LOQ) and linear dynamic range (LDR) values derived from the calibration plot, are summarized in Table 3.9. LOQ value was calculated as 17.3 µM, based on 10 δ/m where δ is the standard deviation of the blank and m is the slope of the calibration curve [31]. DSP-AuNPs@SER probe can be used successfully for the determination of Neu5Ac above 17.3 µM levels.

Table 3.9 The statistical data obtained from calibration plot in Figure 3.25

Calibration curve equation	**R^2**	**LOQ (µM)**	**LDR (µM)**
y=0.0061x+0.6583	0.995	17.3	17.3-58.3

3.9 Selectivity Studies

3.9.1.1 Selectivity of EDC/NHS-AuNPs@SER Probe Towards Neu5Ac

After adding the same volume of 0.1 mM Neu5Ac, 10 mM of each sugar and all sugar mixture (the final concentration was 10 mM) into the EDC/NHS-AuNPs@SER aliquots, their absorption spectra were collected. Figure 3.26 illustrates their absorption spectra and the color of the solutions.

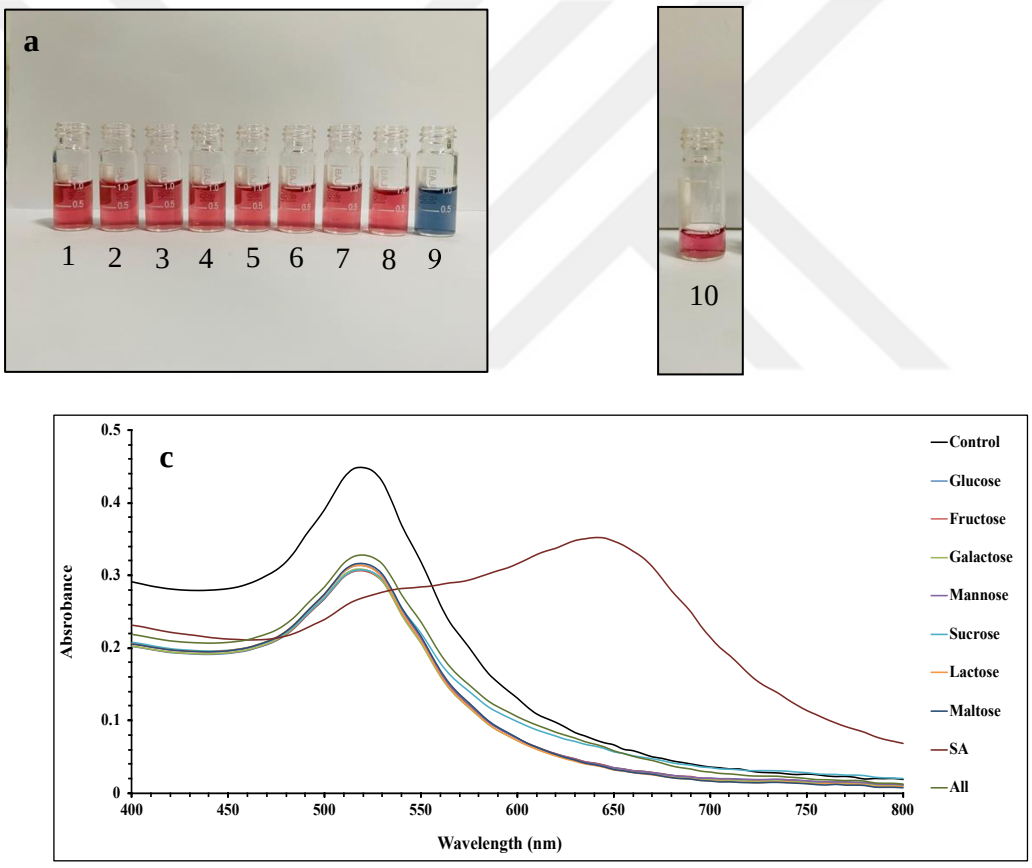


Figure 3.26 (a)The color of change EDC/NHS-AuNPs@SER probe under the influence of sugars (glucose-1, fructose-2, galactose-3, mannose-4, sucrose-5, lactose-6 and maltose-7, respectively), sialic acid-9 and under the influence of sialic acid and mixture of sugars (All-10) (b)UV-Vis absorption spectra of EDC/NHS-AuNPs@SER probe under the influence of sugars, sialic acid and mixture of sugars

Figure 3.26 shows the colors and absorbance spectra of EDC/NHS-AuNPs@SER nanoparticles in different sugar media and N-acetylneuraminic acid standard solution. As seen in Figure 3.26(a), the red to blue color change only occurs in the N-acetylneuraminic acid solution of the EDC/NHS-AuNPs@SER nanoparticles, meaning that the probe interacts only with Nue5Ac and does not respond to sugar molecules. This is also evident from the absence of the second peak in the absorbance spectra of simple sugar solutions containing EDC/NHS-AuNPs@SER nanoparticles. The expected peak shift occurs only for the N-acetylneuraminic acid solution of nanoparticles as shown in Figure 3.26(b). These observations indicate the specific selectivity of the prepared probe to N-acetylneuraminic acid among the selected sugars.

Figure 3.27 illustrates the bar graph of the absorbance ratios ($A_{625}/A5_{21}$) of EDC/NHS-AuNPs@SER nanoparticles in different sugar solutions, in N-acetylneuraminic acid standard solution, and mixture solutions of all sugars. The vertical lines correspond to the high and low absorbance ratios measured in different media. Thus, the bar graph visually shows the difference in absorbance ratios of AuNPs@SER nanoparticles measured in N-acetylneuraminic acid solution and various sugar solutions.

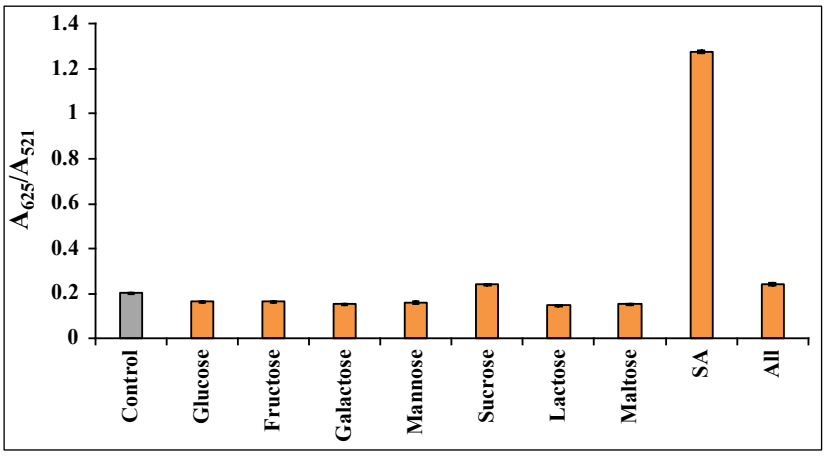


Figure 3.27 Absorbance ratio of EDC/NHS-AuNPs@SER under the influence of different sugars, SA, and the mixture of sugars (All)

As shown in Figure 3.27, the absorbance ratios of nanoparticles in sugar solutions are equal to or lower than the absorbance ratio of the control solution. On the contrary, the absorbance ratio in the presence of Neu5Ac is sevenfold higher than that of the sugar solutions. Consequently, the bar graph makes it easier to see the selectivity of AuNPs@SER nanoparticles to Neu5Ac compared to selected simple sugars.

3.9.1.2 Selectivity of DSP-AuNPs@SER Probe Towards Neu5Ac

After adding the same volume of 0.1 mM Neu5Ac, 10 mM of each sugar and all sugar mixture (the final concentration was 10 mM) into the DSP-AuNPs@SER aliquots, their absorption spectra were collected. Figure 3.28 illustrates their absorption spectra of these solutions.

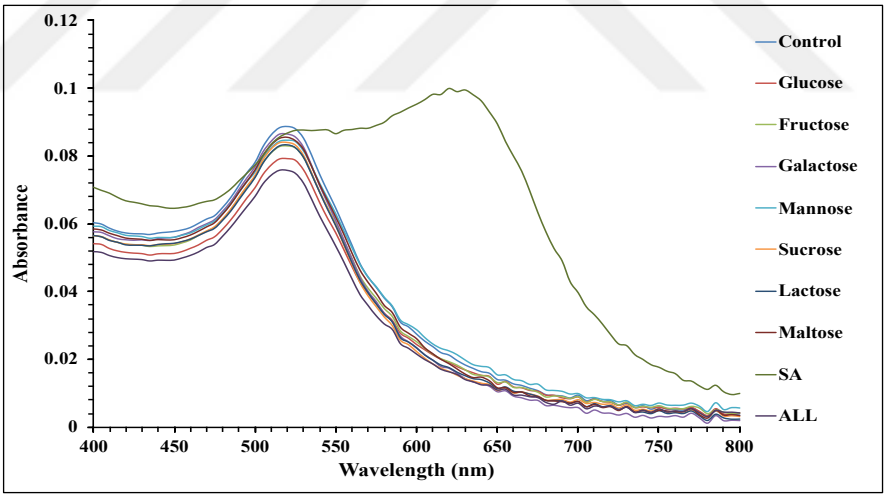


Figure 3.28 Absorption spectra of DSP-AuNPs@SER probe under the influence of sugars, sialic acid and mixture of sugars

Figure 3.29 (a) shows the colors of EDC/NHS-AuNPs@SER nanoparticles in different sugar media and N-acetylneuraminic acid standard solution. The red to blue color change only occurs in the N-acetylneuraminic acid solution of the DSP-

AuNPs@SER nanoparticles, meaning that the probe interacts only with Nue5Ac and does not respond to other sugar molecules. This is also evident from the absence of the second peak at 625 nm in the absorbance spectra of simple sugar solutions containing DSP-AuNPs@SER nanoparticles. Figure 3.29 (b) illustrates the bar graph of the absorbance ratios ($A_{625}/A5_{21}$) of DSP-AuNPs@SER nanoparticles in different sugar solutions, in N-acetylneuraminic acid standard solution, and mixture solutions of all sugars. The vertical lines correspond to the highest and lowest absorbance ratios measured in different media. Thus, the bar graph visually shows the difference in absorbance ratios of AuNPs@SER nanoparticles measured in N-acetylneuraminic acid solution and various sugar solutions.

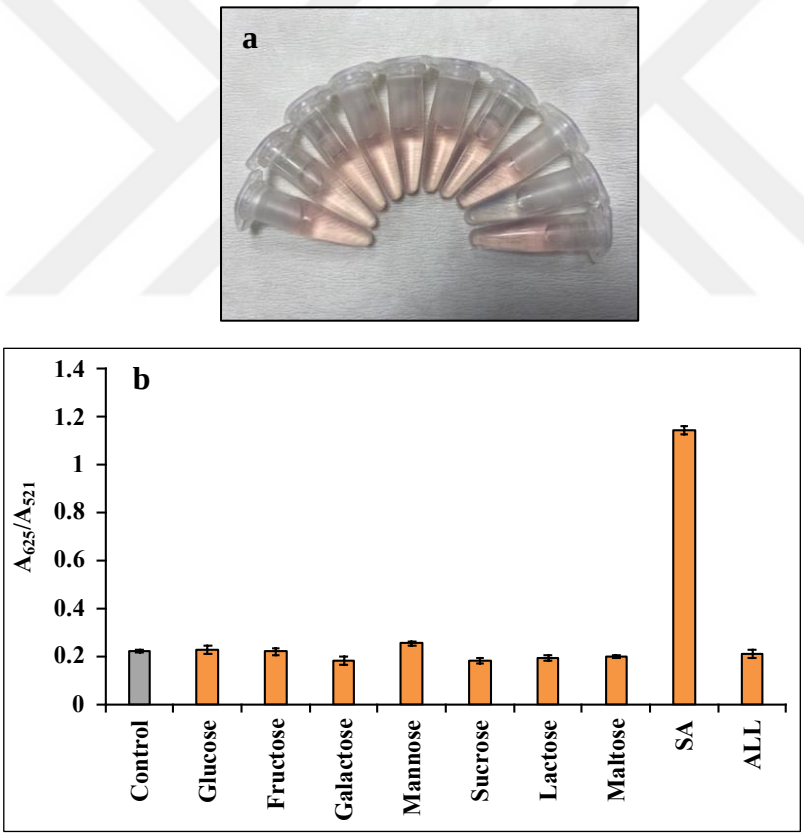


Figure 3.29 (a) the color of DSP-AuNPs@SER probe in control, glucose, fructose, galactose, mannose, sucrose, lactose, maltose, SA and mixture of sugars ALL, respectively (b) The bar graph of absorbance ratios (A_{625}/A_{521}) of DSP-AuNPs@SER with different sugars, SA and mixture of sugars (ALL)

CHAPTER 4

CONCLUSION

Sialic acid plays a vital role in mediating and modulating a variety of physiological and pathological activities due to its widespread distribution and location in human body. Most pathogens and toxins bind to sialic acid, since it has unique structural properties. The binding of pathogens and toxins to sialic acid changes sialic acid concentration in human body. Even the slightest change in sialic acid concentration signal pathological conditions. Hence, the quantification of sialic acid is significant for early detection of many diseases.

Serotonin is a crucial neurotransmitter to carry signals between the nerve cells throughout the body. It controls the sensory information in the central nervous system. Moreover, Serotonin has a specific affinity to sialic acid. Affinity of Serotonin to sialic acid provides an advantage for sialic acid determination. Hence, Serotonin was used as a ligand in this study.

The colorimetric methods with gold nanoparticles have an advantage as probe for a wide range of analytes due to their unique optical and electronic properties. Furthermore, it has many other advantages such as simplicity, speed, and low-cost. In particular, the naked eye color transitions of gold nanoparticles provide great simplification of colorimetric detection.

For the determination of sialic acid, the sialic acid sensor was used basically based on the aggregation of functionalized gold nanoparticles. The citrate stabilized gold nanoparticles were functionalized by using EDC/NHS coupling based on ligand exchange reaction. Serotonin was assembled on functionalized gold nanoparticles by the amine coupling reaction. Different sialic acid concentrations were added gradually to this nanoparticle solution. Furthermore, citrate stabilized gold nanoparticles were functionalized by using DSP crosslinker in order to increase the

sensitivity of sialic acid sensor. Similarly, progressive additions of different sialic acid concentrations resulted in aggregation of serotonin modified gold nanoparticles.

The one of the differences between two probes is the incubation time. The incubation time was chosen by measuring the reaction time. It was investigated by monitoring the aggregation in the presence of different concentrations of Neu5Ac by UV-Vis spectrophotometer. The absorption spectra were collected, and the incubation time was chosen according to the results of absorbance ratio (A_{650}/A_{521}). It can be concluded that DSP probe works faster when compared to the EDC/NHS one. The limit of quantification 257.5 μM was calculated for Neu5Ac by using EDC/NHS-AuNPs@SER probe. The limit of quantification 10.0 μM was calculated for Neu5Ac by using DSP-AuNPs@SER probe. The limit of quantification 17.3 μM was calculated for Neu5Gc by using DSP-AuNPs@SER probe. The normal range of total sialic acid (TSA) level in serum/plasma is 1.58-2.22 mM whereas the free form of Neu5Ac only constituting 0.5-3 μM. SA levels are elevated accordingly to the type disease. Thus, both EDC/NHS-AuNPs@SER and DSP-AuNPs@SER colorimetric probe is appropriate for SA detection.

The selectivity was studied by comparing the response of both EDC/NHS-AuNPs@SER and DSP-AuNPs@SER probes under the influence of various sugar molecules. These sugars have similar chemical structures with sialic acids in terms of their hydroxyl groups. Only sialic acid provided a color change on probes. Probes are highly selective for sialic acid determination in the presence of other biomolecules, even if in the presence of mixture of all sugars.

Humans lack N-glycolylneuraminic acid. However, N-glycolylneuraminic acid can be found in human body due to certain types of diseases. The increase in the total sialic acid amount in human serum is usually correlated with cancer. Hence, both quantification and identification of sialic acid is significant for early detection of cancer. The aim of separation of N-acetylneuraminic acid and N-glycolylneuraminic acid experiments was used to find the concentrations of N-acetylneuraminic acid and N-glycolylneuraminic acid from the concentration of total sialic acid. The studies on

the separation of them are continuing. The determination of total concentration of sialic acid in human serum will be studied by using DSP-AuNPs@SER probe and the finding of both N-acetylneuraminic acid and N-glycolylneuraminic concentration will be studied, as a future work.

REFERENCES

[1] S. Bayda, M. Adeel, T. Tuccinardi, M. Cordani, and F. Rizzolio, "The history of nanoscience and nanotechnology: From chemical-physical applications to nanomedicine," *Molecules*, vol. 25, no. 1. MDPI AG, 2020.

[2] Y. S. Mary, C. Yohannan Panicker, T. Varghese, and S. Sebastian, "Nanoscience and nanotechnology-A review," *Oriental Journal of Chemistry*, vol. 26, no. 3, pp. 901-910, 2010.

[3] I. Khan, K. Saeed, and I. Khan, "Nanoparticles: Properties, applications and toxicities," *Arabian Journal of Chemistry*, vol. 12, no. 7. Elsevier B.V., pp. 908–931, 2019.

[4] C. T. J, S. Shikha, and R. Ramesh, "Nanotechnology: Interdisciplinary science of applications," *African Journal of Biotechnology*, vol. 12, no. 3, pp. 219–226, 2013.

[5] J. Krajczewski, K. Kołątaj, and A. Kudelski, "Plasmonic nanoparticles in chemical analysis," *RSC Advances*, vol. 7, no. 28. Royal Society of Chemistry, pp. 17559–17576, 2017.

[6] M. Kim, J. H. Lee, and J. M. Nam, "Plasmonic Photothermal Nanoparticles for Biomedical Applications," *Advanced Science*, vol. 6, no. 17. John Wiley and Sons Inc., 2019.

[7] H. Yu, Y. Peng, Y. Yang, and Z. Y. Li, "Plasmon-enhanced light–matter interactions and applications," *npj Computational Materials*, vol. 5, no. 1. Nature Publishing Group, 2019.

[8] V. Amendola, R. Pilot, M. Frasconi, O. M. Maragò, and M. A. Iatì, "Surface plasmon resonance in gold nanoparticles: A review," *Journal*

of Physics Condensed Matter, vol. 29, no. 20. Institute of Physics Publishing, 2017.

[9] X. Y. Liu, J. Q. Wang, C. R. Ashby, L. Zeng, Y. F. Fan, and Z. S. Chen, "Gold nanoparticles: synthesis, physiochemical properties and therapeutic applications in cancer," *Drug Discovery Today*, vol. 26, no. 5. Elsevier Ltd, pp. 1284–1292, 2021.

[10] F. Compostella, O. Pitirollo, A. Silvestri, and L. Polito, "Glyco-gold nanoparticles: Synthesis and applications," *Beilstein Journal of Organic Chemistry*, vol. 13. Beilstein-Institut Zur Forderung der Chemischen Wissenschaften, pp. 1008–1021, 2017.

[11] A. K. Khan, R. Rashid, G. Murtaza, and A. Zahra, "Gold nanoparticles: Synthesis and applications in drug delivery," *Tropical Journal of Pharmaceutical Research*, vol. 13, no. 7. University of Benin, pp. 1169–1177, 2014.

[12] S. Alex and A. Tiwari, "Functionalized gold nanoparticles: Synthesis, properties and applications-A review," *Journal of Nanoscience and Nanotechnology*, vol. 15, no. 3, pp. 1869–1894, 2015.

[13] J. Shan and H. Tenhu, "Recent advances in polymer protected gold nanoparticles: Synthesis, properties and applications," *Chemical Communications*, no. 44. Royal Society of Chemistry, pp. 4580–4598, 2007

[14] J. Das and H. Yang, "Enhancement of electrocatalytic activity of DNA-conjugated gold nanoparticles and its application to DNA detection," *Journal of Physical Chemistry C*, vol. 113, no. 15, pp. 6093–6099, 2009.

[15] L. Zhao, Y. Wang, Z. Li, Y. Deng, X. Zhao, and Y. Xia, "Facile synthesis of chitosan-gold nanocomposite and its application for

exclusively sensitive detection of Ag+ ions," *Carbohydrate Polymers*, vol. 226, 2019.

[16] J. Xu, Y. Hu, S. Wang, X. Ma, and J. Guo, "Nanomaterials in electrochemical cytosensors," *Analyst*, vol. 145, no. 6. Royal Society of Chemistry, pp. 2058–2069, 2020.

[17] B. Ahmad, N. Hafeez, S. Bashir, A. Rauf, and Mujeeb-ur-Rehman, "Phytofabricated gold nanoparticles and their biomedical applications," *Biomedicine and Pharmacotherapy*, vol. 89. Elsevier Masson SAS, pp. 414–425, 2017.

[18] K. Zhang, T. Zeng, X. Tan, W. Wu, Y. Tang, and H. Zhang, "A facile surface-enhanced Raman scattering (SERS) detection of rhodamine 6G and crystal violet using Au nanoparticle substrates," *Applied Surface Science*, vol. 347, pp. 569–573, 2015.

[19] J. H. Lee, H. Y. Cho, H. K. Choi, J. Y. Lee, and J. W. Choi, "Application of gold nanoparticle to plasmonic biosensors," *International Journal of Molecular Sciences*, vol. 19, no. 7. MDPI AG, 2018.

[20] T. L. Doane and C. Burda, "The unique role of nanoparticles in nanomedicine: Imaging, drug delivery and therapy," *Chemical Society Reviews*, vol. 41, no. 7, pp. 2885–2911, 2012.

[21] M. Elbahri, S. Homaeigohar, and M. A. Assad, "Reflective Coloration from Structural Plasmonic to Disordered Polarizonic," *Advanced Photonics Research*, vol. 2, no. 7, p. 2100009, 2021.

[22] M. T. Rahman and E. v. Rebrov, "Microreactors for gold nanoparticles synthesis: From faraday to flow," *Processes*, vol. 2, no. 2. MDPI AG, pp. 466–493, 2014.

[23] B. John Turkevich, P. Cooper Stevenson, and J. Hillier, " A Study of the Nucleation and Growth Processes in the Synthesis of Colloidal Gold," Discuss. Faraday Soc., vol. 11, no. c, pp. 55-75, 1951.

[24] W. Cai, T. Gao, H. Hong, and J. Sun, "Applications of gold nanoparticles in cancer nanotechnology," *Nanotechnology, Science and Applications*, vol. 1, pp. 17-32, 2008.

[25] T. J. Jayeoye, W. Cheewasedtham, C. Putson, and T. Rujiralai, "Colorimetric determination of sialic acid based on boronic acid-mediated aggregation of gold nanoparticles," *Microchimica Acta*, vol. 185, no. 2018.

[26] S. Ghosh, "Sialic acid and biology of life: An introduction," in *Sialic Acids and Sialoglycoconjugates in the Biology of Life, Health and Disease*, Elsevier, pp. 1–61, 2020.

[27] A. N. Samraj *et al.*, "Polyclonal human antibodies against glycans bearing red meat-derived non-human sialic acid N-glycolylneuraminic acid are stable, reproducible, complex and vary between individuals: Total antibody levels are associated with colorectal cancer risk," *PLoS ONE*, vol. 13, no. 6, 2018.

[28] S. M. Levonis, J. Pittet, B. C. M. Pointon, and S. S. Schweiker, "Combining versatility with cost-effectiveness: Determination of both free and bound sialic acids, N-acetylneuraminic and N-glycolylneuraminic in unprocessed bovine milk," *Journal of Chromatography B: Analytical Technologies in the Biomedical and Life Sciences*, vol. 1104, pp. 130–133, 2019.

[29] X. Zhou, G. Yang, and F. Guan, "Biological Functions and Analytical Strategies of Sialic Acids in Tumor," *Cells*, vol. 9, no. 2. NLM (Medline), Jan. 22, 2020.

[30] A. Varki, “Sialic acids in human health and disease,” *Trends in Molecular Medicine*, vol. 14, no. 8. pp. 351–360, Aug. 2008.

[31] T. J. Jayeoye, W. Cheewasedtham, C. Putson, and T. Rujiralai, “A selective probe based on 3-aminophenyl boronic acid assembly on dithiobis(succinimidylpropionate) functionalized gold nanoparticles for sialic acid detection in human serum,” *Journal of Molecular Liquids*, vol. 281, pp. 407–414, 2019.

[32] “Eur J Clin Investigation - 2001 - Sillanaukee - Occurrence of sialic acids in healthy humans and different disorders”.

[33] R. O’kennedy *et al.*, “A critical analysis of the use of sialic acid determination in the diagnosis of malignancy,” 1991.

[34] M. A. Crook, P. Tutt, H. Simpson, and J. C. Pickup, “,1 ~,11 R %1 II %111 I1 I’1 ll! I’~111 R’~ IRI I ~,%1),” 1993.

[35] X. Zhou, G. Yang, and F. Guan, “Biological Functions and Analytical Strategies of Sialic Acids in Tumor,” *Cells*, vol. 9, no. 2. NLM (Medline), 2020.

[36] Z. Zhang, M. Wuhrer, and S. Holst, “Serum sialylation changes in cancer,” *Glycoconjugate Journal*, vol. 35, no. 2. Springer New York LLC, pp. 139–160, 2018.

[37] L. Skoza and S. Mohos, “Stable Thiobarbituric Acid Chromophore with Dimethyl Sulphoxide. Application to Sialic Acid Assay in Analytical De-o-acetylation, ” *Biochem. J.*, vol. 159, pp. 457-462, 1976.

[38] A. K. Shukla and R. Schauer, “Fluorimetric Determination of Unsubstituted and 9(8)-O-Acetylated Sialic Acids in Erythrocyte Membranes,” *Physiol. Chem.*, vol. 363, pp. 255-262, 1982.

[39] J. S. Rohrer, J. Thayer, M. Weitzhandler, and N. Avdalovic, “Analysis of the N-acetylneuraminic acid and N-glycolylneuraminic acid contents of glycoproteins by high-pH anion-exchange chromatography with pulsed amperometric detection,” *Glycobiology*, vol. 8, pp. 25-43, 1998.

[40] D. C. Hurum and J. S. Rohrer, “Five-minute glycoprotein sialic acid determination by high-performance anion exchange chromatography with pulsed amperometric detection,” *Analytical Biochemistry*, vol. 419, no. 1, pp. 67–69, 2011.

[41] S. Hara, M. Yamaguchi, Y. Takemori, M. Nakamljra, and Y. Ohkura, “Highly Sensitive Determination of N-acetyl and N-glycolyneuraminic Acids in Human Serum and Urine and Rat Serum by Reversed-Phase Liquid Chromatography with Fluorescence Detection,” *J. Chromatogr. B Biomed*, vol. 377, pp. 111-119, 1986.

[42] S. Hara, Y. Takemori, M. Yamaguchi, M. Nakamura, and Y. Ohkura, “Fluorometric High-Performance Liquid Chromatography of N-Acetyl-and A/-Glycolylneuraminic Acids and Its Application to Their Microdetermination in Human and Animal Sera, Glycoproteins, and Glycolipids’,” *Anal. Biochem*., vol. 164, pp. 138-145, 1987.

[43] A. Kawabata, N. Morimoto, Y. Oda, M. Kinoshita, R. Kuroda, and K. Kakehi, “Determination of mucin in salivary glands using sialic acids as the marker by high-performance liquid chromatography with fluorometric detection,” *Analytical Biochemistry*, vol. 283, no. 1, pp. 119–121, 2000.

[44] Q. U. A. Zahra, Z. Luo, R. Ali, M. I. Khan, F. Li, and B. Qiu, “Advances in gold nanoparticles-based colorimetric aptasensors for the detection of antibiotics: An overview of the past decade,” *Nanomaterials*, vol. 11, no. 4. MDPI AG, 2021.

[45] M. H. Jazayeri, T. Aghaie, A. Avan, A. Vatankhah, and M. R. S. Ghaffari, "Colorimetric detection based on gold nano particles (GNPs): An easy, fast, inexpensive, low-cost and short time method in detection of analytes (protein, DNA, and ion)," *Sensing and Bio-Sensing Research*, vol. 20. Elsevier B.V., pp. 1–8, 2018.

[46] S. Sankoh, C. Thammakhet, A. Numnuam, W. Limbut, P. Kanatharana, and P. Thavarungkul, "4-mercaptophenylboronic acid functionalized gold nanoparticles for colorimetric sialic acid detection," *Biosensors and Bioelectronics*, vol. 85, pp. 743–750, 2016.

[47] T. K. Smith, K. J. Park, and G. W. Hennig, "Colonic migrating motor complexes, high amplitude propagating contractions, neural reflexes and the importance of neuronal and mucosal serotonin," *Journal of Neurogastroenterology and Motility*, vol. 20, no. 4. Journal of Neurogastroenterology and Motility, pp. 423–446, 2014.

[48] H. Y. Meltzer, "The Importance of Serotonin-Dopamine Interactions in the Action of Clozapine," *British Journal of Psychiatry*, vol. 160, no. 17, pp. 22-29, 1992.

[49] D. Keszthelyi, F. J. Troost, and A. A. M. Masclee, "Understanding the role of tryptophan and serotonin metabolism in gastrointestinal function," *Neurogastroenterology and Motility*, vol. 21, no. 12. pp. 1239–1249, 2009.

[50] V. Rut, V. Heleen, B. Jozef V., "Serotonin, serotonin receptors and their actions in insects," *Neurotransmitter*, 2015.

[51] E. L. M. Ochoa and A. D. Bangham, "N-acetylneuraminic Acid Molecules as Possible Serotonin Binding Sites," J. Neurochem., vol. 26, no. 6, pp. 1193-1198, 1976.

[52] M. Meininger *et al.*, "Sialic acid-specific affinity chromatography for the separation of erythropoietin glycoforms using serotonin as a

ligand," *Journal of Chromatography B: Analytical Technologies in the Biomedical and Life Sciences*, vol. 1012–1013, pp. 193–203, 2016.

[53] K. Kazukai, K. Mitsuhiro, and M. Yuki, "Process for Producing sugar Chain Derivative, Structure Analysis Method, and Sugar Chain Derivative," United States Patent, No: US 8,318,694 B2, 2012.

[54] P. Tengvall, E. Jansson, A. Askendal, P. Thomsen, and C. Gretzer, "Preparation of multilayer plasma protein films on silicon by EDC/NHS coupling chemistry," *Colloids And Surfaces B: Biointerfaces*, vol. 28, no. 4, pp. 261-272, 2003.

[55] S. Durocher, A. Rezaee, C. Hamm, C. Rangan, S. Mittler, and B. Mutus, "Disulfide-linked, gold nanoparticle based reagent for detecting small molecular weight thiols," *J Am Chem Soc*, vol. 131, no. 7, pp. 2475–2477, 2009.

[56] C. Amgoth *et al.*, "Solvent assisted size effect on AuNPs and significant inhibition on K562 cells," *RSC Advances*, vol. 9, no. 58, pp. 33931–33940, 2019.

[57] B. Yang *et al.*, "Size-Controlled Green Synthesis of Highly Stable and Uniform Small to Ultrasmall Gold Nanoparticles by Controlling Reaction Steps and pH," *Journal of Physical Chemistry C*, vol. 121, no. 16, pp. 8961–8967, 2017.

[58] D. B. Grys *et al.*, "Citrate Coordination and Bridging of Gold Nanoparticles: The Role of Gold Adatoms in AuNP Aging," *ACS Nano*, vol. 14, no. 7, pp. 8689–8696, 2020.

[59] X. Liu, M. Atwater, J. Wang, and Q. Huo, "Extinction coefficient of gold nanoparticles with different sizes and different capping ligands," *Colloids and Surfaces B: Biointerfaces*, vol. 58, no. 1, pp. 3–7, 2007.

[60] M. J. E. Fischer, “Amine coupling through EDC/NHS: a practical approach.,” *Methods Mol Biol*, vol. 627, pp. 55–73, 2010.

[61] W. Y. Wahlgren *et al.*, “Substrate-bound outward-open structure of a Na+-coupled sialic acid symporter reveals a new Na+ site,” *Nature Communications*, vol. 9, no. 1, 2018.

[62] J. C. Mohan, G. Praveen, K. P. Chennazhi, R. Jayakumar, and S. v. Nair, “Functionalised gold nanoparticles for selective induction of in vitro apoptosis among human cancer cell lines,” *Journal of Experimental Nanoscience*, vol. 8, no. 1, pp. 32–45, 2013.

[63] L. Zhang, Y. Cheng, J. Lei, Y. Liu, Q. Hao, and H. Ju, “Stepwise chemical reaction strategy for highly sensitive electrochemiluminescent detection of dopamine,” *Analytical Chemistry*, vol. 85, no. 16, pp. 8001–8007, 2013.

[64] A. Lagutschenkov, J. Langer, G. Berden, J. Oomens, and O. Dopfer, “Infrared spectra of protonated neurotransmitters: Serotonin,” *Journal of Physical Chemistry A*, vol. 114, no. 50, pp. 13268–13276, 2010.